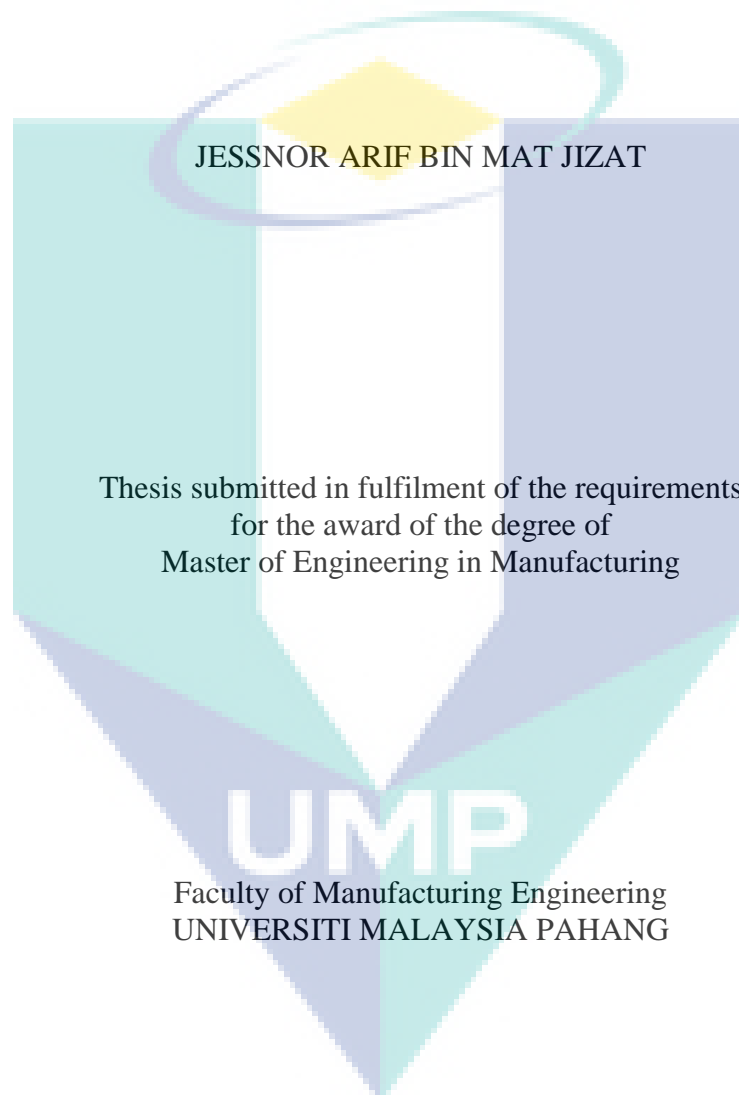


LANDMARK GUIDED TRAJECTORY OF AN AUTOMATED GUIDED VEHICLE
USING OMNIDIRECTIONAL VISION



SEPTEMBER 2014

UNIVERSITI MALAYSIA PAHANG

DECLARATION OF THESIS AND COPYRIGHT

Author's full name : Jessnor Arif bin Mat Jizat
 Date of birth : 14 February 1983
 Title : Landmark Guided Trajectory of an Automated Guided Vehicles
 using Omnidirectional Camera
 Academic Session : 2013/2014

I declare that this thesis is classified as:

- CONFIDENTIAL** (Contains confidential information under the Official Secret Act 1972)*
- RESTRICTED** (Contains confidential information as specified by the organization where research was done)*
- OPEN ACCESS** I agree that my thesis to be published as online open access (full text)

I acknowledge that Universiti Malaysia Pahang reserve the right as follows:

1. The Thesis is the Property of Universiti Malaysia Pahang
2. The Library of Universiti Malaysia Pahang has the right to make copies for the purpose of research only.
3. The Library has the right to make copies of the thesis for academic exchange.

Certified By:

 (Student's Signature)

830214-10-5127

New IC/ Passport Number

Date: 11 September 2014

 (Signature of Supervisor)

Prof. Dr. Zahari Taha

Name of Supervisor

Date: 11 September 2014

SUPERVISOR'S DECLARATION

I hereby declare that I have checked this thesis and in my opinion, this thesis is adequate in terms of scope and quality for the award of the degree of Master of Engineering in Manufacturing.

Signature

Name of Supervisor: PROF.DR ZAHARI TAHA

Position: PROFESOR

Date: 11 SEPTEMBER 2014



STUDENT'S DECLARATION

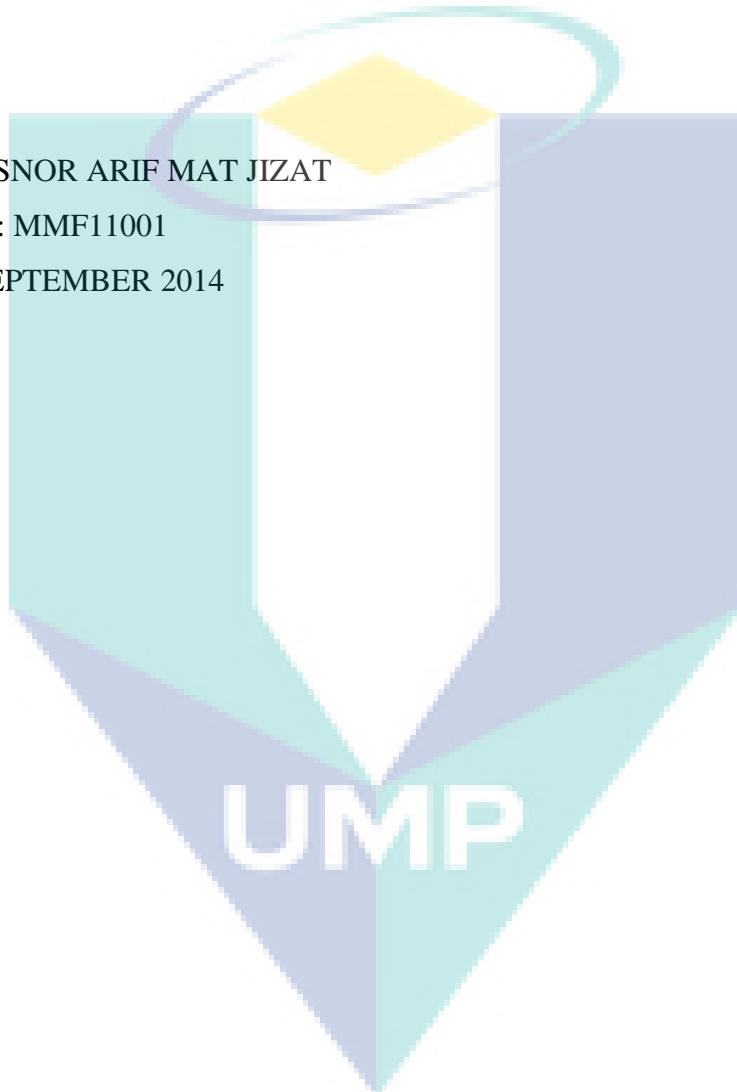
I hereby declare that the work in this thesis is my own except for quotations and summaries which have been duly acknowledged. The thesis has not been accepted for any degree and is not concurrently submitted for award of other degree.

Signature

Name: JESSNOR ARIF MAT JIZAT

ID Number: MMF11001

Date: 11 SEPTEMBER 2014



ACKNOWLEDGEMENTS

In the name of Allah the Most Beneficent and Most Merciful,
Abu Hurairah narrated that the Messenger of Allah said :
"Whoever is not grateful to the people, he is not grateful to Allah."
(Jami' at Tirmidhi, Book 27, Hadith 2081)

Alhamdulillah, all praised to Allah, with all His will, I managed to complete this thesis. I would like to take this opportunity to thank people who have help me academically, financially, and emotionally to complete this thesis.

First and foremost I would like to express my deepest gratitude to my supervisor, Professor Dr. Zahari Taha who has guide me with his vast experience and knowledge during my research years. His insight and guidance has allowed me to experience research work at the highest level.

Second, I would like to express my gratitude to my beloved father, Mat Jizat Abdol, and my beloved mother, Norimah Othman, my siblings, Hafiz, Elmy, Eina, and Ezrin, my sister in law Azlina, and my nephew, Syahmi, who provide sanctuary for me to cope with the research work stress.

Third, I would like to acknowledge the contribution of the Dean of Faculty Manufacturing Engineering, Prof. Dr. Wan Azhar Wan Yusoff who has given me the opportunity to further my study under supervision of a dedicated professor and all the support he has given me throughout my study.

Fourth, my appreciation goes to my beloved fiancée, Nashita Ab Razak, who has been very persevere, very understanding and always pushing me to face challenges in order to complete this thesis.

Fifth, to all staff members of Faculty of Manufacturing Engineering that have facilitated the research lab where I conducted my research.

Finally my appreciation goes to all researchers at Innovative Manufacturing, Mechatronics and Sports Lab, without whom, I would not have found joy in the research work. For all your strong and continuous support and encouragement toward the completion of this research, I will be forever indebted to you all.

Jazakallahukhaira

ABSTRACT

The omnidirectional camera is very useful in tracking a landmark for automated guided vehicle (AGV). The omnidirectional camera can sense object 360° around the AGV thus eliminating the need of camera panning or robotic reorientation. The image produced by the omnidirectional camera is usually highly distorted. However, one feature of the image captured by an omnidirectional camera is that the distortion only against the height of the object. Object with negligible height has negligible image distortion. With this feature in mind, this research investigates the trajectory generated from an AGV towards an identified and recognized landmark using omnidirectional camera without rectifying the distortion into perspective view. The research work involves landmark identification and recognition using image processing step. The landmark used, was enlarged to four different sizes, code-128 barcodes with cyan background and red orientation marker. The landmark identification and recognition is processed from the image captured by the omnidirectional camera. The camera was mounted on the AGV and remain as the sole range sensor for the AGV to sense its environment. Three fundamental trajectories used in robotics navigation namely straight, left turn, and right turn were experimented to present the trajectory of an AGV guided by a landmark. The AGV was modelled using Bicycle Model. The trajectory of the AGV is then simulated using MATLAB/Simulink. Next, the simulation work is validated with the experimental work. A proportional control is applied in the experimental work for the AGV move toward the landmark. All experiments were conducted in a laboratory environment with controlled illumination. The work thus demonstrate that the image captured using omnidirectional camera can be used to identify and recognize a landmark without going through any typical omnidirectional image unwarping process into a perspective view. The important navigational information for the vision-based-AGV can be extracted directly from the camera feed.

The logo for UMP (Universiti Malaysia Perlis) is a large, stylized letter 'V' shape. It is composed of four triangular segments meeting at a central point. The top-left and bottom-right segments are light blue, while the top-right and bottom-left segments are light green. The letters 'UMP' are printed in white, bold, sans-serif font across the center of the 'V' shape.

UMP

ABSTRAK

Kamera semua arah adalah amat berguna dalam mengesan suatu mercu tanda untuk kenderaan automatik terpandu (AGV). Kamera ini berupaya mengesan objek 360° di sekeliling kenderaan tersebut seterusnya menghapuskan keperluan pergerakan kamera atau orientasi semula robot. Imej yang terhasil daripada kamera semua arah ini biasanya sangat herot-benyot. Walaubagaimanapun, satu ciri imej yang herotan terhasil oleh kamera semua arah ini hanya melibatkan ketinggian objek. Objek yang mempunyai ketinggian boleh abai mempunyai herotan yang boleh diabaikan juga. Oleh itu penyelidikan ini dijalankan bagi menyelidik trajektori AGV tersebut bagi pergerakan ke arah suatu mercu tanda yang telah dikenalpasti tanpa membetulkan herotan itu kepada perspective camera. Penyelidikan ini menggunakan langkah pemprosesan imej bagi mengenalpasti suatu mercu tanda. Mercu tanda yang digunakan adalah empat jenis saiz kod bar (code-128) yang telah dibesarkan. Mercu tanda ini menggunakan warna latar sian dan tanda orientasi merah. Proses pengenalanpastian dilakukan melalui imej yang ditangkap oleh kamera semua arah. Kamera semua arah tersebut merupakan satu satunya sensor julat bagi AGV tersebut untuk mengecam persekitarannya. Tiga pergerakan trajektori asas dalam navigasi robot, gerakan lurus, belok kanan dan belok kiri, telah diujikaji. AGV tersebut menggunakan model basikal dan telah disimulasi melalui perisian MATLAB/Simulink. Kemudian, kerja kerja simulasi ini telah disahkan melalui kerja kerja ujikaji. Kawalan berkadaran digunakan dalam kerja-kerja ujikaji ini. Kesemua ujikaji dilakukan dalam persekitaran makmal dengan kawalan pencahayaan. Kerja penyelidikan ini berjaya menunjukkan bahawa imej yang diambil menggunakan kamera semua arah, walaupun mempunyai herotan, tetap masih boleh digunakan untuk proses pengenalanpastian dan pengecaman mercu tanda tanpa pembedahan herotan tersebut.

The logo of Universiti Malaysia Perlis (UMP) is a large, stylized letter 'V' shape. The left side of the 'V' is light blue, the right side is light green, and the bottom point is a darker blue. The letters 'UMP' are written in white, bold, sans-serif font across the center of the 'V'.

TABLE OF CONTENTS

	Page
TITLE PAGE	i
DECLARATION OF THESIS AND COPYRIGHT	ii
SUPERVISOR'S DECLARATION	iii
STUDENT'S DECLARATION	iv
ACKNOWLEDGEMENTS	v
ABSTRACT	vi
ABSTRAK	vii
TABLE OF CONTENTS	viii
LIST OF TABLES	xi
LIST OF FIGURES	xii
LIST OF SYMBOLS	xv
LIST OF ABBREVIATIONS	xvii
CHAPTER 1 INTRODUCTION	
1.0 Introduction	1
1.1 Research Background	2
1.2 Problem Statement	3
1.3 Research Objectives	4
1.4 Scope of Study	4
1.5 Methodology of the Study	5
1.6 Concept Definition and Research Terminology	7
1.7 Organization of the Thesis	9
CHAPTER 2 LITERATURE REVIEW	
2.0 Introduction	10
2.1 Vision-based Automated Guided Vehicles	11
2.1.1 Vision-based Automated Guided Vehicle Camera	13

2.2	Landmarks for Navigation	15
2.2.1	Natural or Artificial Landmarks	16
2.3	Path Planning with Landmark for the Mobile Robot Trajectory	18
2.4	Vision-based AGV Control	19
2.5	Chapter Summary	20
CHAPTER 3	RESEARCH METHODOLOGY: MODELLING OF THE AGV	
3.0	Introduction	21
3.1	AGV Model	21
3.2	Moving to a Pose	26
3.2.1	Non-Holonomic Constraint	26
3.2.2	Position and Orientation	27
3.3	Moving with Camera Perspective	28
3.4	Controlling the AGV Movement	30
3.5	Chapter Summary	32
CHAPTER 4	RESEARCH METHODOLOGY: EXPERIMENTAL SETUP	
4.0	Introduction	33
4.1	Assembly of the AGV with Omnidirectional Camera	33
4.1.1	The AGV Platform	33
4.1.2	The Omnidirectional Camera and Its Holder	34
4.1.3	The Microcontroller and Communication	35
4.1.4	The Image Processing Software	36
4.1.5	The Assembly	37
4.1.6	The Side-slip test	38
4.2	Identifying Detecting and Recognizing Landmarks For the AGV Using Omnidirectional Camera	38
4.2.1	The Landmarks	38
4.2.2	Static Detection Experiment Setup	39
4.2.3	In-Motion Detection Experiment Setup	40

4.3	Trajectory Generation for Alignment with The Landmark	41
4.3.1	Image to Object Mapping	42
4.3.2	Image Processing by Roborealm	44
4.4	Chapter Summary	47
CHAPTER 5 RESULT AND DISCUSSION		
5.0	Introduction	48
5.1	Side Slip Test of AGV	48
5.2	Landmark Detection	53
5.2.1	Result of Static Test	53
5.2.2	In-motion Experiment	55
5.3	Trajectory Path Experiment	58
5.3.1	Straight trajectory	58
5.3.2	Right Turn Experiment	60
5.3.3	Left Turn Experiment	63
5.3.4	Discussion of Trajectory Experiment	65
5.4	Chapter Summary	66
CHAPTER 6 CONCLUSION AND FUTURE WORK		
6.1	Summary of Research Work	67
6.2	Future Work	68
REFERENCES		70
APPENDICES		
A	Statistics Data Calculation for the Trajectories	74
B	On-Board AGV Arduino Program	76
C	Roborealm CScript Program	77
D	List of Publications	79

LIST OF TABLES

Table No	Title	Page
2.1	Artificial landmarks used in navigation and its detection method	17
4.1	Result of image mapping by ratio method on the omnidirectional camera.	43
5.1	Result of experiments for with barcodes placed on the side of AGV.	54
5.2	Result of experiments for landmark placement on AGV's front or rear.	55
5.3	Result for landmark detection while AGV is in motion	56

A large, semi-transparent watermark logo for UMP (Universitas Muhammadiyah Purwokerto) is centered on the page. The logo consists of a shield-like shape divided into four quadrants by a white cross. The top-left and bottom-right quadrants are light blue, while the top-right and bottom-left quadrants are light purple. The letters 'UMP' are written in a bold, white, sans-serif font across the center of the shield.

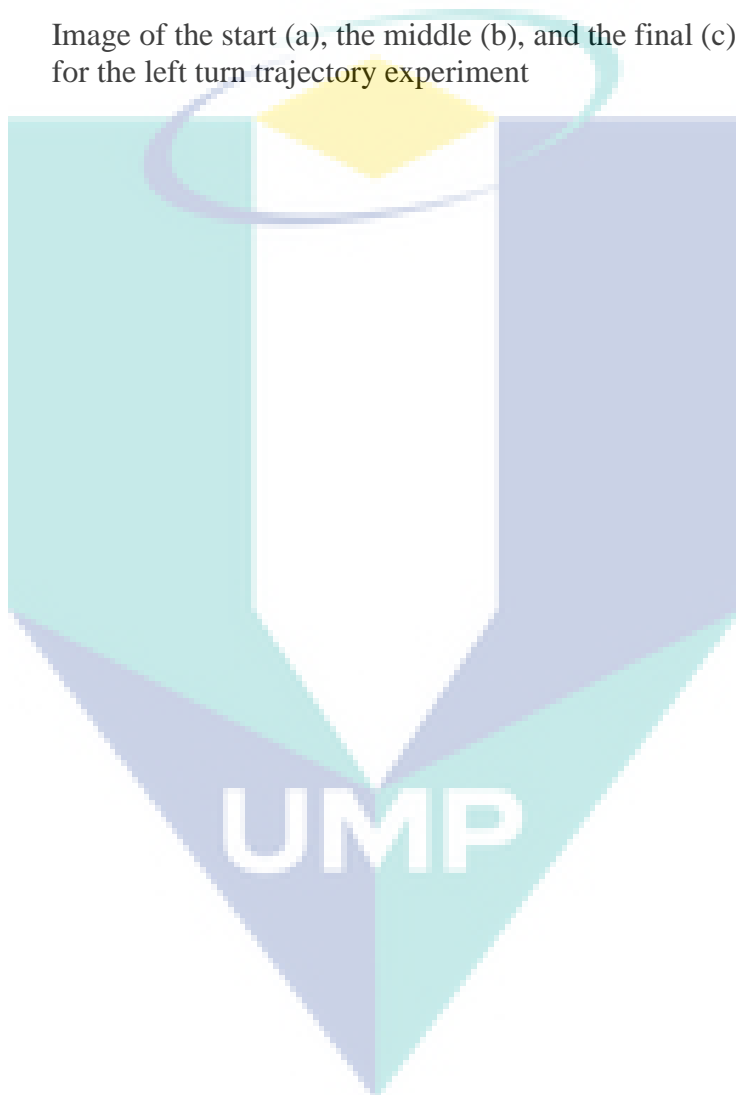
UMP

LIST OF FIGURES

Figure No.	Title	Page
1.1	Overview of the research methodology using Waterfall model	6
2.1	Generic system architecture for AGV	12
2.2	Omnidirectional camera lens	14
3.1	Skeleton sketch of the four wheels AGV	22
3.2	Front axle connected to the front servo	23
3.3	Bicycle model of the AGV	24
3.4	AGV in a global coordinates	27
3.5	On-board omnidirectional camera view	28
3.6	Simplified Block diagram for the feedback control of the AGV	30
3.7	MATLAB/Simulink block diagram for the AGV controller.	32
4.1	(a) The AGV dimensions (b) Front-axle motor (c) Servo motor for front axle.	34
4.2	Omnidirectional camera used in this research	34
4.3	Partial programming code for the AGV	36
4.4	Roborealm GUI	37
4.5	The final assembly of the AGV	37
4.6	The barcode use in this study	39
4.7	Sample of barcodes size tested in this experiments	39
4.8	Position of the landmark standing up (a) and flat on the floor (b)	40
4.9	Experimental setup for trajectory test	41

Figure No.	Title	Page
4.10	Image to object mapping test on omnidirectional camera	42
4.11	Local and global view from the cameras	43
4.12	Image Sequences of the Image Processing and Its Effect to the Image	45
4.13	Mosaic Module User Interface	47
5.1	Comparison between simulation and experiment of direct input manoeuvre	49
5.2	Input pulse for figure 5.1.	49
5.3	Simulation result of varying steering angle.	51
5.4	Input pulse for varying steering angle. (a) 8° left (b) 6° left (c) 4° left (d) 2° left.	52
5.5	Simulation result of varying the duration of steering angle.	52
5.6	Input signal for variable duration of steering angle. a) 3 seconds, b) 2 seconds c) 1.5 seconds, d) 1 second.	53
5.7	Detected and recognized barcode from the image. (a) Standing up barcode size A1. (b) Laying down barcode size A1.	54
5.8	(a) Barcode size A1 place in front of the AGV. (b) Barcode size A1 place on the side of the AGV.	54
5.9	Comparison of the image barcode quality in static mode: (a) A1 size (b) A2 size (c) A3 size (d) A4 size	56
5.10	Comparison of the straight trajectory between the simulation and experiment	58
5.11	Image of the start (a), the middle (b) and the final (c) position for the straight trajectory experiment.	59
5.12	Comparison of the right turn trajectory between the simulation and experiment	61

Figure No.	Title	Page
5.13	Image of the start (a), the middle (b), and the final (c) position for the right turn trajectory experiment.	62
5.14	Comparison of the left turn trajectory between the simulation and experiment.	63
5.15	Image of the start (a), the middle (b), and the final (c) position for the left turn trajectory experiment	64



LIST OF SYMBOLS

α_f	Resultant front steering angle of the AGV.
α_r	Resultant rear steering angle of the AGV.
r	Turning radius of the AGV.
β	Heading angle of the AGV
X	Horizontal position of the AGV.
Y	Vertical position of the AGV.
w_e	The distance between AGV's longitudinal axis to left wheel.
w_g	The distance between AGV's longitudinal axis to right wheel.
γ_{fe}	Steering angle of the left front wheel.
γ_{fg}	Steering angle of the right front wheel.
γ_{re}	Steering angle of the left rear wheel.
γ_{rg}	Steering angle of the right rear wheel.
v	Actual speed of the AGV.
v_f	The front wheel velocity.
v_r	The rear wheel velocity.
δ	Side slip angle of the AGV.
l_f	Distance between the AGV's Centre of Gravity and front axle.
l_r	Distance between the AGV's Centre of Gravity and rear axle.
\dot{X}	Horizontal speed of the AGV.
\dot{Y}	Vertical speed of the AGV.
$\dot{\beta}$	Heading angular speed of the AGV.
v_t	Front and rear speed
ρ	Shortest distance between the AGV and the landmark.
τ	The angle between horizontal line and ρ .
σ	The angle of the AGV longitudinal axis and ρ .
θ	The angle of ρ to the AGV longitudinal axis at the final pose.
T_a	Transformation angle between the local coordinates system and the global coordinates system
τ_c	The angle between horizontal line and ρ , measured by camera.
X^*	Output of the X position proportional control

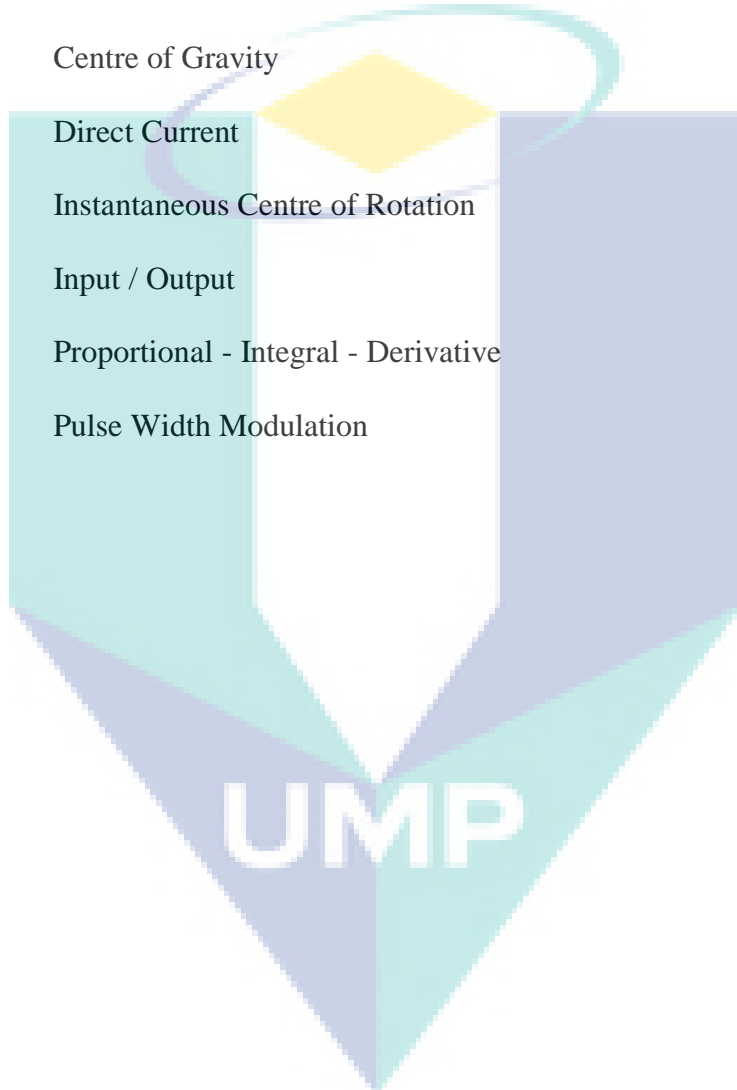
Y^*	Output of the Y position proportional control
TP_x	Target X-Position of the AGV
TP_y	Target Y-Position of the AGV
CP_x	Current X-Position of the AGV
CP_y	Current Y-Position of the AGV
K_p	Proportional Gain for ρ
σ^*	Output of the σ proportional control
θ^*	Output of the θ proportional control
TO_β	Target Orientation of the AGV
CO_β	Current Orientation of the AGV
K_θ	Proportional gain for θ
K_σ	Proportional gain for σ
RSE	Residual Sum Square Error
VAR	Statistical Variance
$STDEV$	Statistical Standard Deviation
n	Number of Data
Y_{exp}	Corresponding Y Position at an X Position in Experiment
Y_{sim}	Corresponding Y Position at an X Position in Simulation



UMP

LIST OF ABBREVIATIONS

1D	One Dimensional
2D	Two dimensional
AGV	Automated Guided Vehicle
CoG	Centre of Gravity
DC	Direct Current
ICR	Instantaneous Centre of Rotation
IO	Input / Output
PID	Proportional - Integral - Derivative
PWM	Pulse Width Modulation



CHAPTER 1

INTRODUCTION

1.0 INTRODUCTION

On extra-large facilities such as ports, warehouses, or production factories, a conventional method (conveyor belts, trucks) of material handling system may not be practical. Automated guided vehicle (AGV) usually is a typical choice for the companies to manage the material handling system. AGVs can provide support in the form of material or product delivery from one station to another. The AGVs can drive directly to the designated station and skip the unnecessary stations.

AGV can be defined as an unmanned, autonomous vehicle that is a subset of mobile robots. The AGV may have on-board computer to store path planning and motion control system. A traditional AGV usually rely on either wired technology, guided tape, laser technology or inertial guidance systems that make use of the gyroscopes and wheel odometry for their path planning system (Kelly et al., 2007). These technologies have made the AGVs dependent on the infrastructure in order to navigate around the facilities where it was deployed. The dependency on the infrastructure demands every single AGV to be in operational state to avoid any disruption to the whole system. This system is, more or less, similar to a conveyor belt system.

Later generations of AGV are able to deviate significantly from their guide path. This type of AGV is usually known as a free ranging AGV and employs perception system on-board. The perception system, path planning and motion control are the common intelligent systems embedded in an AGV in order for it to carry out its assigned task in a manufacturing plant.

In a span of more than 50 years of AGV development, various sensors have been utilised in order to improve the AGV perception system. Among the sensors being used

are optical sensor, sonar sensor, magnetic sensor, laser sensor, Global Positioning System (GPS) and camera based vision system (Xie, 1995). The perception system should provide the information for the AGV regarding the position of the target, current location of the AGV with respect to its origin and possible obstacles in its path. As an AGV's working environment becomes more complex, a reduction in perception process time is desired in order for the AGV to cope with its designated task.

Recent advancement in computer vision led to a rising interest on camera sensors for an AGV's perception system (Miljković et al., 2013). Apart from its economical reason, using camera for perception allows more information to be extracted within a single sensor. Obstacle avoidance, path planning, visual-servoing, and object recognition are among the navigation protocols executed from images acquired by the camera system.

The technology allows more researches being conducted in order to understand the robotics perception from a simple range sensor to self-localization and mapping. Furthermore, the camera configuration, such as monocular (Sabikan et al., 2010) binocular, (Xu and Tian, 2011) trinocular (Xie, 1995) or omnidirectional camera (Weijia et al., 2008), also contributes to the application of camera systems in robotics.

1.1 RESEARCH BACKGROUND

In order to develop a free ranging AGV, the AGV needs to have at least an algorithm to localize itself within its environment. The localization can be achieved by several methods such as Simultaneous Localization and Mapping, range laser or sonar and triangulation, map building, or landmarks. Navigation by using landmarks can be useful in manufacturing warehouses. The landmarks can simultaneously be treated as machine or station identification for the company asset management. The landmarks should be placed in a global coordinate system, thus giving the AGV the localization needed to complete its required navigation. Navigation by known landmarks permits the AGV to directly approach the landmarks instead of having to follow a specific line around the facilities.

Adopting a camera in an AGV system allows the AGV to identify landmarks placed in a manufacturing environment through image processing. Camera has been extensively used as part of AGV perception due to its flexibility and superior image quality. However, a frontal camera has certain limitation mainly a small view angle. In

order to provide a full 360° view around the AGV, a frontal camera system have to be panned or tilted. Panning and tilting mechanism adds extra weight to the AGV and will cause a slight delay in identifying the location of the landmarks. These limitations will in turn limit the capability of the AGV to interact with its environment.

In order to get a full 360° view around the AGV, an omnidirectional camera is usually used. The omnidirectional camera view can be achieved by using fisheye lens, or catadioptric camera system. Catadioptric camera system is a camera with spherical, conical, hyperboloidal or parabolical mirror system with the main purpose of extending their field of view. However, the images captured by omnidirectional camera are usually highly distorted.

1.2 PROBLEM STATEMENT

The current issue on the AGV's vision system is the narrow field of view (Taha et al., 2010). The narrow field of views present a limitation to the infrastructure-free AGV to manage its path trajectory, landmark recognition and obstacle identification especially when the landmarks are frequently out of the camera field of view.

Weijia et al used a fisheye lens to detect coloured landmark beacon for their AGV navigation (Weijia et al., 2008). Before the recognition is made, they ran an image rectification process in order to get a correlation between the fisheye image points and the real images. The image rectification process refers to the step of unwarping omnidirectional image into a perspective image view before any other image processing steps to extract usable information from the image are applied.

Yingjie et al utilised a catadioptric omnidirectional camera system in a highly dynamic environment for their mobile robot (Yingjie et al., 2004). They tracked landmarks in the form of a goal post or corner post for the mobile robot localization. They rectified the image through a process named cylindrical projection to eliminate the robot and the ceiling from the view. This rectification process causes significant reduction in image data for navigational approach. In both, the approaches rectification of the image is necessary thus slowing down the navigation process.

Taha et al discovered that image captured by catadioptric omnidirectional camera only distort significantly against the height of an object. The object length and width on the ground distortion, when viewed from the camera system, is negligible. (Taha et al., 2010)

Thus, the rectification of the image captured by the omnidirectional camera leads toward reduction of data, longer image processing time, and consumed more computing power. However, there exists certain parts on the image where the distortion is negligible.

1.3 RESEARCH OBJECTIVES

It is hypothesized that the AGV can identify and recognize a landmark and navigate to approach the landmark using omnidirectional camera without going through any image rectification process. Therefore, the aim of this research is to develop an AGV navigation system using catadioptric omnidirectional camera without any image rectification. The navigation system should include landmark recognition and identification, and trajectory generation.

In order to achieve the research aim, three objectives are set namely:

- (i) To develop a system using catadioptric omnidirectional camera as the range sensor for an AGV
- (ii) To identify and recognize landmarks for navigation using the developed system.
- (iii) To generate the trajectory for the AGV to align and position itself with a landmark using the developed system.

1.4 SCOPE OF THE STUDY

The main focus of this study is landmark recognition and the AGV navigation toward the landmark. Contributing factors for AGV navigation using landmark are identified and described in this research. These factors include modelling of four-wheel steering with a four-wheel drive AGV, omnidirectional catadioptric camera as a sole sensor on board the platform, target recognition and detection and target approach by the AGV. In this research several requirements are identified for the design of the landmarks.

The landmarks are easily reproduced from off-the-shelf material with minimal modification.

However, the study is conducted in a controlled environment. The experimental test did not run in a real factory warehouse. The experiment did not take into account the integration between the AGV and the material handling system in a manufacturing environment. The AGV used in this research is only applicable to AGV locomotive as it does not tow any material behind the platform.

Furthermore, the study only focuses on the algorithm for landmark recognition and the AGV's navigation towards the landmark. No obstacle avoidance algorithm, or battery management algorithm were embedded into the algorithm used in this research. The landmark used in this study was artificial landmark and specific to the code-128 only.

In addition, the camera used to identify and recognition of the landmark was an omnidirectional camera which consist of a perspective camera pointing upward and a parabolical mirror on top of the camera at the focal point. The experiment also assumes that the landmarks are clearly visible to the AGV camera system and there are no obstructions, partially or otherwise, between the AGV's camera and the landmark.

In order to control the AGV autonomously from its current position towards the landmark, proportional control is applied to the AGV microcontroller. The error is generated from the difference of the landmark position (set point) and the current AGV position. The tuning of the proportional gains was by the trial and error method. Only proportional control is used because the primary concern was to generate the trajectory for the AGV to align and position itself with a landmark. Then, only three trajectories were examined in this study namely straight trajectory, right turn trajectory, and left turn trajectory.

1.5 METHODOLOGY OF THE STUDY

The research work was conducted in four phases, namely modelling, assembly, manual test, and autonomous test phase. Following a waterfall model concept, each phase must be satisfactorily conducted before moving on to the next phase. Figure 1.1 shows an overview of the research activities using a Waterfall model for the projects implementation.

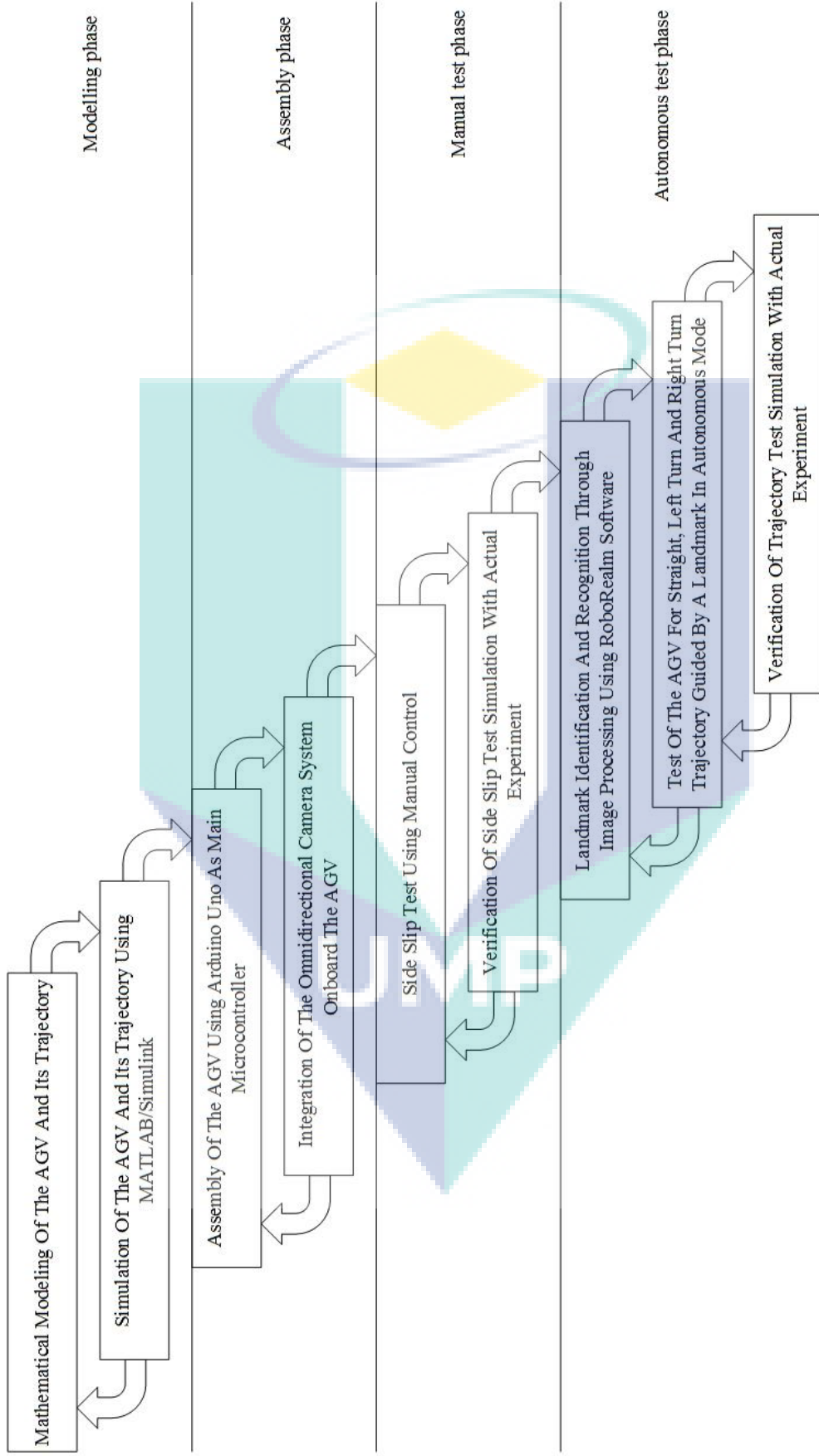


Figure 1.1: Overview of the research methodology using Waterfall model.

The modelling phase focused on the simulation of the derived mathematical model using MATLAB/Simulink while in the assembly phase the main focus was on establishing a wireless radio frequency connection signal between the AGV's on board camera system and the workstation so that the image feed from the camera can be processed on the workstation. Results from the image processing provided the control signals for the AGV on board microcontroller to move the AGV using Bluetooth connection.

In the manual test phase, the AGV was controlled manually to evaluate the AGV behaviour and validate the mathematical model simulation. After that, the research continued by identifying and recognizing the proposed landmark and run experiments for the straight, left turn and right turn trajectories. Then, the simulation results for the three trajectories were validated against the experimental results.

1.6 CONCEPT DEFINITION AND RESEARCH TERMINOLOGY

This section will explain several terms that are used throughout this thesis which may have ambiguous definitions to the reader. Among the term used are:

(i) Vision-based automated guided vehicle (AGV)

Vision-based AGV refers to an autonomous mobile robot that incorporate camera as a sensor to scan its environment. The camera system can either be active or passive, single or multiple configurations. The information extracted from the camera vision plays a significant role in the AGV operation.

(ii) Omnidirectional camera or omnidirectional image

Omnidirectional camera used in this research refers to a camera system that consists of an ordinary perspective camera and a parabolical mirror. Objects are reflected on the mirror before being captured by the ordinary perspective camera. The image generated from this camera system is called an omnidirectional image.

(iii) Natural or artificial landmark

Landmarks are distinctive feature discovered from the images captured by the camera to help the AGV navigation process. If the landmark is gathered from the environment without purposely placed in the surrounding, the landmark is considered a natural landmark, whereas if the feature is purposely placed in the surrounding, the landmark is called an artificial landmark.

(iv) Localization

Localization is a technique for determining the AGV position in global coordinate reference frame. Global coordinate reference frame is a reference frame given by the Cartesian axes for the entire environment where the AGV operates whereas the local coordinate reference frame may refer to the Cartesian axes with respect to the specific moving object such as AGV local coordinate system or camera local coordinate system

(v) Trajectory

Trajectory refers to a path taken by the AGV to move towards a landmark either by mathematical calculation or visual clues gathered by the AGV's range sensor.

(vi) Station

Station is a theoretical place, where the landmark is placed and the AGV make a good transfer from or to the AGV.

1.7 ORGANIZATION OF THE THESIS

This thesis is arranged as follows:

Chapter 1 presents the background of the study, problem statement, research objectives, scope of the study and clarification of terms used in this thesis.

Chapter 2 describes a review of related works that has been conducted prior to this thesis. Three main issues are reviewed in this chapter mainly vision based AGVs, landmark recognition and its detection methods, and path planning with the landmark for mobile robot navigation.

Chapter 3 explains the methodology used in this research in order to identify and recognize the landmark and gathering data from the AGV actual path. This includes the description of image processing steps for landmark recognition and path planning.

Chapter 4 discusses the AGV trajectory using mathematical model of the four-wheel steering and four-wheel drive AGV and mathematical model of the generated path on which the AGV should follow towards the landmarks.

Chapter 5 discusses the data from the experiments and compares with the calculated simulation of the generated path. The deviation of experimental data from the simulation is then justified.

Chapter 6 presents the concluding remarks, knowledge gained and future works recommendation.

CHAPTER 2

LITERATURE REVIEW

2.0 INTRODUCTION

This chapter is a review of past work from other researchers. There are three main issues being reviewed in this chapter mainly vision based AGVs (AGV), landmark recognition and its detection methods, and path planning with landmark for the mobile robot trajectory. These issues are relevant to the research objectives as presented in Chapter 1.

Early AGV utilises physical guide path such as line, wire or radio signals buried in the ground. The intelligent system was built on the ground instead of onto the AGV itself. This kind of system is known as a fixed path AGV. In recent years AGVs have begun to employ microcomputer on-board. This change allows the navigation system of the AGV to have more control in terms of route selection, obstacle avoidance, and velocity control in order to navigate around its operational area. The later generation of AGV is more susceptible to modification of operations such as changes of flow, new station or equipment change (Martínez-Barberá and Herrero-Pérez, 2010).

With the application of contactless technology such as ultrasonic (Ratner and McKerrow, 2003, Tong et al., 2005, Yan et al., 2006), laser (Golnabi, 2003, Guo et al., 2013, Yu et al., 2013) or vision (Aixue et al., 2012, Her et al., 2013) as range sensor, the AGV has become more similar to autonomous mobile robot especially in terms of its navigation system.

2.1 VISION-BASED AUTOMATED GUIDED VEHICLES

Vision based AGV utilises vision sensor and computer image processing for navigation. AGVs may share a common generic architecture where the vehicle is governed by its sensors to gather information from the surrounding and respond to its surrounding by several actuators. Information processed from the vehicle's sensors is called perception. The perception can be in the form of image processing to get usable information for path planning and control when the vehicle is using a camera as its sensor.

Figure 2.1 shows the generic system architecture of an AGV. The level of complexity for each block depends on the environment where the vehicle operates. The higher the environment complexity, the more sensors may be needed to complement each other for robust and reliable motion control of the vehicle (Ilas, 2013).

A review by DeSouza and Kak revealed that researches on vision based AGV for indoor navigation can be classified into three main groups namely map-based-navigation, map-building based navigation, and mapless-navigation. The first group is map-based-navigation where the AGV depends on a system based on a topological map of the environment or a user-created map by modelling the environment where the AGV will operate. The second group is map-building based navigation where the AGV is equipped with a system that constructs its own geometric or topological representation for its navigation and the third group employs mapless-navigation where the AGV uses no explicit representation about the operational environment. It makes use of the visual images cue to recognize objects in the surrounding to determine a collision-free navigation path. (DeSouza and Kak, 2002)

Although the review by DeSouza and Kak is focused mainly on AGV researches before the year 2000, their main classification seems to guide more recent researches. A more recent review by Guzel (Güzel, 2013) and Bonin-Font (Bonin-Font et al., 2008) also featured researches in the same classification.

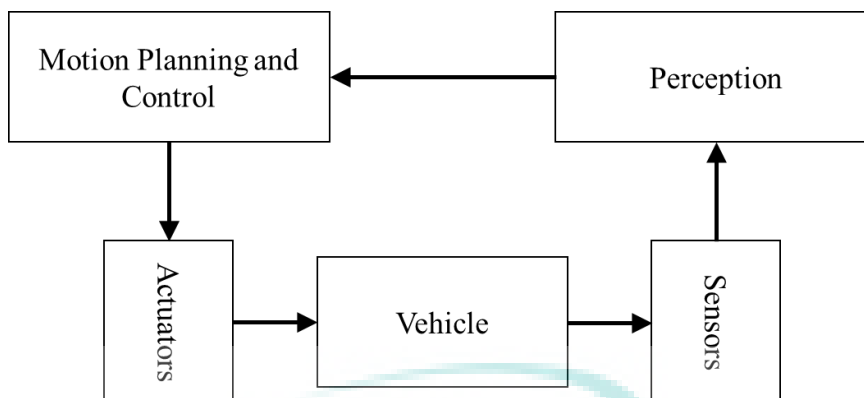


Figure 2.1: Generic system architecture for AGV

Source: (Ilas, 2013)

Bonin-Font et al. however combined the map based navigation and map building navigation into a single category: map-navigation systems. They then elaborate the division into three more subdivisions namely metric map-using system, metric map-building system, and topological map-based system (Bonin-Font et al., 2008). Metric map-using system requires a complete map to be available for the AGV's computer to make a decision while metric map-building system creates a map as the AGV navigates and build upon existing information whenever new information for the map becomes available. The AGV can navigate even with partially known map. Topological map-based system using nodes and linkage between node where the nodes represent interesting places for navigation and the linkage may represent time or distance.

Guzel highlighted recent trends and state of the art technology for AGV especially mapless-navigation for indoor environment. (Güzel, 2013). However, Guzel underlined two common approaches for map-based navigation AGV. The first is metric based maps which can produce optimum result for indoor navigation and the second is more qualitative methods that utilised recognizable landmarks to generate a suitable path for the AGV.

It is interesting to note that while Guzel classified the navigation by using landmarks under map based navigation system, Bonin-Font et al, however classified it under mapless navigation system. The different classification may arise due to the usage of landmarks in robotics navigation. On one hand, the landmarks are used for place recognition where the robot explores its surrounding and matches up its whereabouts in

a topological map (Mata et al., 2001). On the other hand, the landmarks are used to provide navigation clues for the robot between initial position and the target position without depending on a prior known map (Zhang et al., 2012). A further review on landmarks navigation will be discussed in later section.

2.1.1 Vision-Based Automated Guided Vehicle Camera.

The adoption of a camera on a mobile robot for visual navigation was started by Moravec with the “Stanford Cart” (Moravec, 1983). The cart was used to drive through cluttered environment autonomously using images broadcasted by its on-board camera system. The cart moved from an initial position to a specified final position while avoiding any object it deemed as obstacle. The path planning was solely based on the images it acquired. The Stanford cart then became a pioneer on AGV research. Since then research on vision autonomous vehicle continues to gather interest even until recent times.

The most common choice of camera in AGV research is a monocular camera (Congiu et al., 1994, Jin Woo et al., 2002, Jun et al., 2008, Kay and Luo, 1993, Kelly et al., 2007, Petriu et al., 1993, Ping et al., 2006). It is usually cheaper and smaller in size compared to other camera setups. However, images gathered from a monocular camera do not have depth information. Some image algorithm (T.Taylor, 2004) or image mapping by calculation (Taha and Jizat, 2012) is therefore needed to gain range information.

Since the range information can be determined by calculation, image from a monocular camera can be used for perception without image pre-processing needed such as image aligning with binocular camera and image unwarp with omnidirectional camera. This will allow computing overhead to be concentrated on image classification for decision making in motion control.

On the other hand, stereo vision (binocular camera) has the advantage of depth information. Depth information allows for much easier measurement of distance from the camera. This measurement of distance then may be used for AGV triangulation among visible landmarks (Cucchiara et al., 2007), obstacle distance for obstacle avoidance algorithm (Spampinato et al., 2013), or 3D map building algorithm (Songmin et al., 2011).

Binocular camera setup employs two similar cameras in parallel to create disparity in order to gather depth information from the images. Thus, binocular camera setup requires complex calibration procedure between the two cameras in order to create images with accurate depth information. This calibration steps can clearly be seen in several other researches (Buxton et al., 1991, Knight and Reid, 2000, Storjohann et al., 1990). It shows that the calibration procedures is a crucial step when dealing with stereo vision and cannot be omitted from the vision algorithm.

Apart from that, another type of camera setup used on AGV is omnidirectional camera. Omnidirectional camera offers an extended field of view of 360° along the horizontal line with one camera rather than a monocular camera or multi-camera setup. The 360° view is created using a circular cone-like reflective lens as shown in Figure 2.2. This extended field of view may obtain much more information from it images such as bearing information, AGV localization, or artificial landmarks recognition (Lee et al., 2008).

The omnidirectional camera wide field of view allows the vision system to recognize landmarks more faster as no tilting, panning or AGV reorientation is needed (Taha et al., 2010). Although the image range may be shorter than perspective camera, the omnidirectional camera can capture image range that is more relevant for robotics navigation.

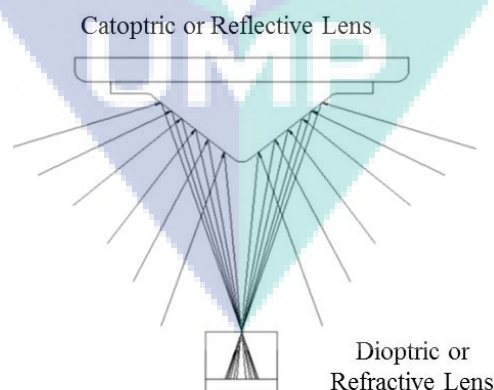


Figure 2.2: Omnidirectional camera lens

Source: (Taha et al., 2010)

Ideally the omnidirectional camera is used for omnidirectional robots where the robot can be driven to all position without changing its orientation. In order to adopt omnidirectional camera to a car-like mobile platform requires a specific algorithm to take into account its constraint as the car-like mobile robot needs to change its orientation frequently for navigation. The adoption of omnidirectional camera as range sensor allows the landmarks that the AGV is tracking to remain in the field of view. This occurrence can be very advantageous for mobile robot navigation. Hence this advantage is the highest criterion in this research.

However, two major disadvantages of using camera as sensor are firstly, the environment in which the AGV is operated must have sufficient illumination. If the required illumination is not fulfilled, the algorithm would definitely fail (Florczyk, 2005). Secondly, the images acquired from the camera contain large information that needs to be filtered before it can be used for navigation control (Florczyk, 2005). The filtering and processing incur significant computer overhead and may affect the AGV's decision making.

2.2 LANDMARKS FOR NAVIGATION

Bonin-Font et al, DeSouza and Kak, Güzel, agreed that the main steps for navigation using landmarks system (Bonin-Font et al., 2008, DeSouza and Kak, 2002, Güzel, 2013) requires a minimum of four steps as follows:

- a) Acquiring image information.
- b) Landmarks detection in current camera view
- c) Matching the landmarks from database
- d) Updating AGV position.

Depending on the AGV setup, the vision sensor usually behaves as a range sensor. The vision allows the AGV's computer to obtain information about its surrounding faster and more reliable as compared to other range sensors. In most cases, some pre-processing are required such as filtering, noise reduction, sharpening, and contrasting when obtaining image information since there may exist certain undesirable feature from the raw images.

The main features of an environment or landmarks can be identified easily using vision sensor and image processing thus increasing flexibility and accuracy. These techniques can thus be applied in all streaming images for almost instantaneous

localization and mapping depending on the capability of the image-processing unit. The same image can also simultaneously be used as obstacle detection and target destination.

Landmark detection in current camera view usually requires further image processing (DeSouza and Kak, 2002). This may include image segmentation, edge detection, thresholding, image morphology, and changing colour depth. The main objective of this step is to extract landmarks from its background.

With the vision focused on the landmarks, the next step is to decode the landmarks and search the computer database for a possible match. If the landmarks matched then the AGV position will be updated. These two steps are very dependent on computer processing performance as the matching and updating process happen at almost on real-time basis.



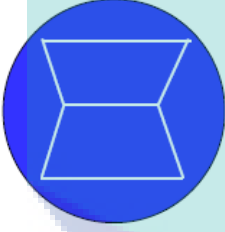
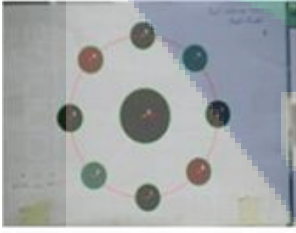
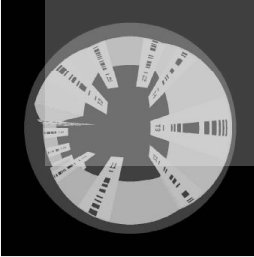

2.2.1 Natural or Artificial Landmarks

For researches in robotics navigation using landmarks, the terms natural landmark or artificial landmark are usually discussed. The term natural landmarks often refers to certain features in the detected environment without placing it purposely in the scene. These features may be door frames, window frames, ceiling lamps or air conditioner vent. After detecting and recognizing the features, the AGV main computer then runs an algorithm to localize itself and then update the AGV position and orientation. This type of landmark navigation may be most useful for map-based-navigation.

On the other hand artificial landmarks may be introduced to the environment in order to assist navigation. The artificial landmarks usually consist of patterns design specifically to assist detection and recognition. The design may include encoded symbols, readable by landmarks detections and recognition algorithms. Table 2.1 shows several landmarks that have been adopted for landmark navigation.

From the sample of artificial landmarks shown in table 2.1, they have several things in common, among others information encoded in the landmarks, orientation of the landmark, and colour or contrast for saliency. These are the considerations when selecting a landmark to be used in this research.

Table 2.1: Artificial landmarks used in navigation and its detection method.

No.	Landmarks	Detection techniques	Reference Source
1		HSI colour space, searching for the square red frame. Form and colour contrast determine the landmarks.	(Zhang et al., 2012)
2		Shape recognition by Canny edge method and Randomized Hough Transform. Image binarization.	(Aixue et al., 2012)
3		HSI colour space. Image segmentation, pixelate block diagram.	(Guanghui and Zhijian, 2011)
4		Hough algorithm and scanning for elliptical shape. Calculate distance for each dot.	(Martín and Adán, 2012)
5		Dominant spatial frequency and edge transition phase using The Discrete Cosine Transform (DCT)	(Fiala, 2004)
6		Matching function through local maximum with linear interpolation to determine inter pixel intensities.	(Briggs et al., 2000)

2.3 PATH PLANNING WITH LANDMARK FOR THE MOBILE ROBOT TRAJECTORY

Siegwart and Nourbakhsh in their book highlight two key competencies for mobile robot path planning (Siegwart and Nourbakhsh, 2004). First, given a map and a goal location, path planning involves identifying a trajectory that will cause the robot to reach the goal location when executed and second, given a real time sensor, an autonomous mobile robot will modify its trajectory in real time to avoid any potential collision.

The work in this thesis however focuses only on the first competency highlighted by Siegwart and Nourbakhsh. Landmarks, for path planning, can be used as target position and orientation as highlighted by Zhang et al. (Zhang et al., 2012). The AGV in a manufacturing warehouse is supposed to align itself with a specific pose to a station. Thus, when a landmark is placed at a station, it is important for the selected landmarks to incorporate orientation. The target position and orientation can be either calculated by software (Chaudhary and Sinha, 2012) or given by detecting a landmark in a topological map. (Jang et al., 2002).

When analysing topological map trajectory from one point to a point (Esparza and Savage, 2013, Lin et al., 2004, Lu et al., 2009), highlighted the patterns that a mobile robot need to accomplish for indoor navigation. The patterns are 90° right turn, 90° left turn, and a straight trajectory. A combination of these patterns can used to navigate a in a mapless navigation.

When a mobile robot navigate from one landmark to another, the in between time can be free ranging as shown by Beinhofer et al. (Beinhofer et al., 2011). The most important navigation step is how the mobile robot aligned itself at the particular landmark, and where is the next landmark orientation relative to the landmark.

2.4 VISION BASED AGV CONTROL

Several control methods are commonly used in vision based AGV control. The methods may include one of the classical control, modern control and artificial intelligence. Classical control drives from error between the target and current parameter, whereas the modern control utilized state space methods. In recent years, artificial intelligence methods such as fuzzy control, artificial neural networks emerges as preferred methods for controlling robotics movement.

A typical classical control utilizes proportional, integral and/or derivative value to adjust the whole system process in order to minimize the error. The classical control often chosen by researchers for its simplicity and reliability. This control method may also provide a fast, stable and robust operation as demonstrated by Ziaie-Rad et al., Xiuzhi Li et al., and Rui Zhao and Jian Fang (Ziaie-Rad et al., 2005, Xiuzhi Li et al., 2012, Rui Zhao and Jian Fang, 2014)

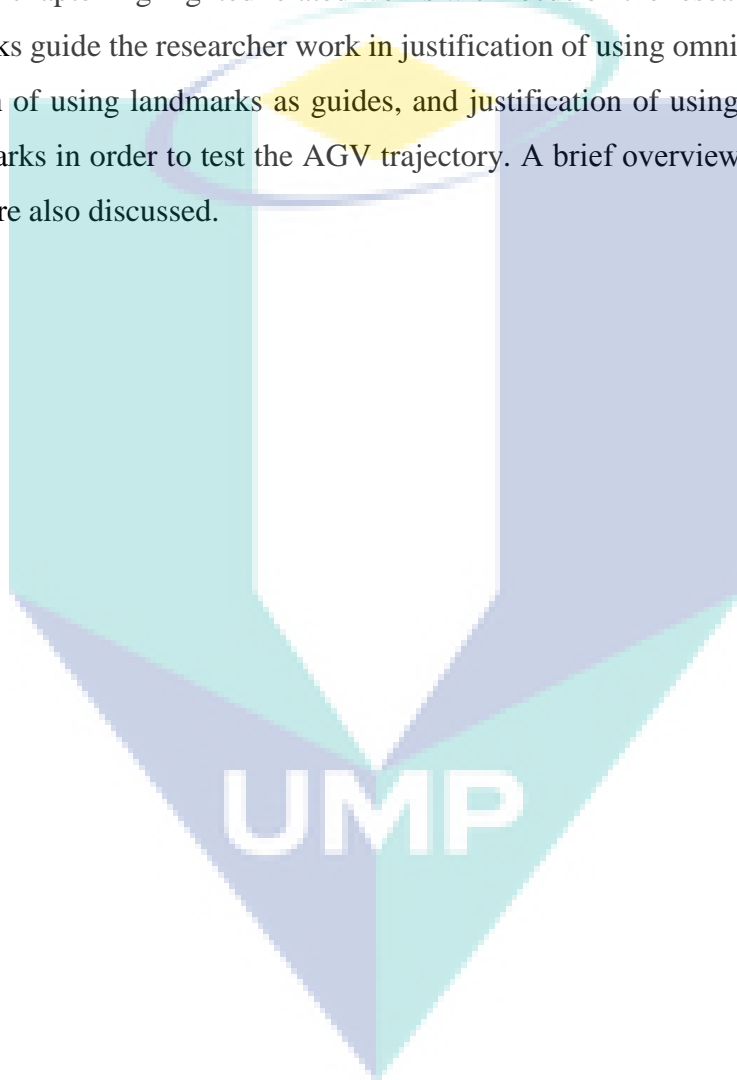
As more sensors were put on board the AGV and the environment where the AGV operates becomes more complex, researchers often opted for state-space method. State space methods helped the AGV learns about its environment in most efficient way as demonstrated by Uchibe et al. (Uchibe et al., 1998) while Andersen et al. showed multiple sensor models including the kinematics and dynamics model of the AGV, vision sensor model, digital encoder model can be combined into state space method for more accurate path tracking AGV using vision feedback. (Andersen et al., 1994).

As the AGV becomes more complex and many uncertain situations emerges from several disturbance parameter, artificial intelligence methods such as fuzzy neural network may be used. The employment of artificial intelligence methods AGV control algorithm allows the AGV to move about its environment with higher precision and sensitivity. The AGV is also more susceptible to several disturbances as well as responding well to the environment especially in tracking object or potential obstacle as demonstrated by Shimizuhira et al. and Huang Hong and Ting Zhang (Shimizuhira et al., 2004, Huang Hong and Ting Zhang, 2009). This usage of fuzzy may also reduce the steady state error generated by classical control algorithm (Chul-Goo Kang and Hee-Sung Kwak, 1996).

In this work, however, a classical control algorithm specifically proportional control was used to control the AGV as the classical control algorithm is robust, simple and reliable and the AGV was operated in a controlled environment inside a laboratory.

2.5 CHAPTER SUMMARY

This chapter highlighted related works with focus on the research objectives. This related works guide the researcher work in justification of using omnidirectional camera, justification of using landmarks as guides, and justification of using trajectory patterns near landmarks in order to test the AGV trajectory. A brief overview on AGV's control algorithm are also discussed.



CHAPTER 3

RESEARCH METHODOLOGY: MODELLING OF THE AGV

3.0 INTRODUCTION

The methodology for achieving the three research objectives were conducted in four phases, modelling of the AGV, assembly of the AGV, manual experiment of the AGV, and autonomous experiment of the AGV. The description for each phases is discussed in two separate chapters. This chapter is focused on a detailed modelling of the AGV. While the next chapter will focused on the assembly of the AGV and the experimental setup. This chapter is organized as follows: AGV model, simulation of AGV motion to a pose, motion with camera perspective and controlling the AGV movement.

3.1 AGV MODEL

The AGV used in this research is a four-wheel drive platform with an all-wheel steering system. Figure 3.1 shows a skeleton sketch of the AGV making a right turn in the global coordinates system. The global coordinate system is fixed to the horizontal plane on which the AGV operates. Several assumptions were made.

Firstly, the position and orientation of the AGV were modelled from the AGV's centre of gravity (CoG). Secondly, the instantaneous centre of rotation point exists outside the system for every turn and the distance between the instantaneous centre of rotation point and the CoG point of the system is the turning radius. Thirdly, the lateral orientation of each tyre must intercept at the instantaneous centre of rotation (ICR) point. Finally, the automated guided vehicle is a rigid body with no slippage on the tyres and on planar motion (Danwei and Feng, 2001).

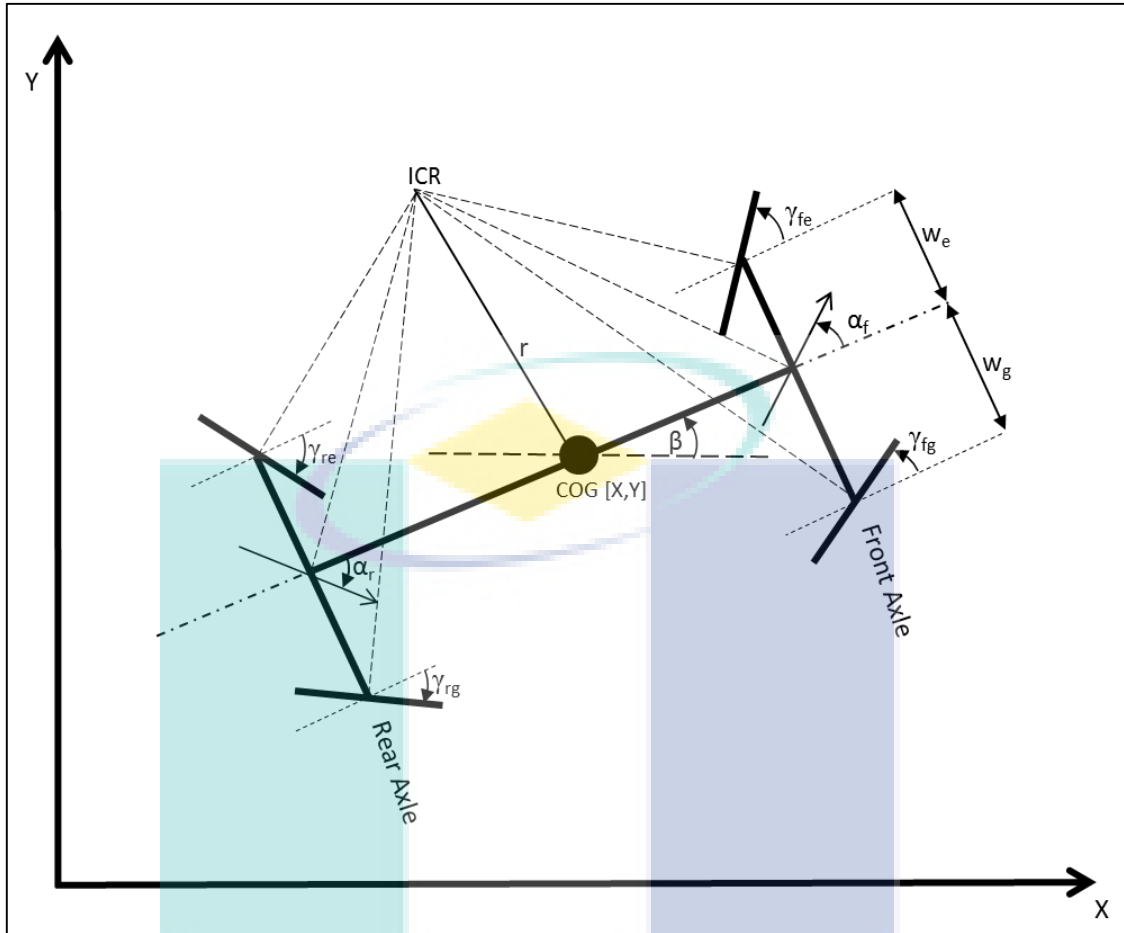


Figure 3.1: Skeleton sketch of the four wheels AGV.

For the purpose of calculation, a global coordinate system X-Y is fixed on the horizontal plane on which the AGV moves. Every angle is considered positive in the counter clockwise direction. Likewise, the velocity is considered positive from left to right as well as from bottom to top. The longitudinal axis of the AGV is a straight reference line along the length of the AGV through its CoG.

The all wheel steering system on the AGV is governed by the pair of wheels on the front and rear axles. Two wheels were mounted on each axle and connected together by a lever. In order to steer the AGV, the lever was pushed by a servo motor either to the left or to the right direction and turned both wheels to a specific angle simultaneously as shown in figure 3.2.

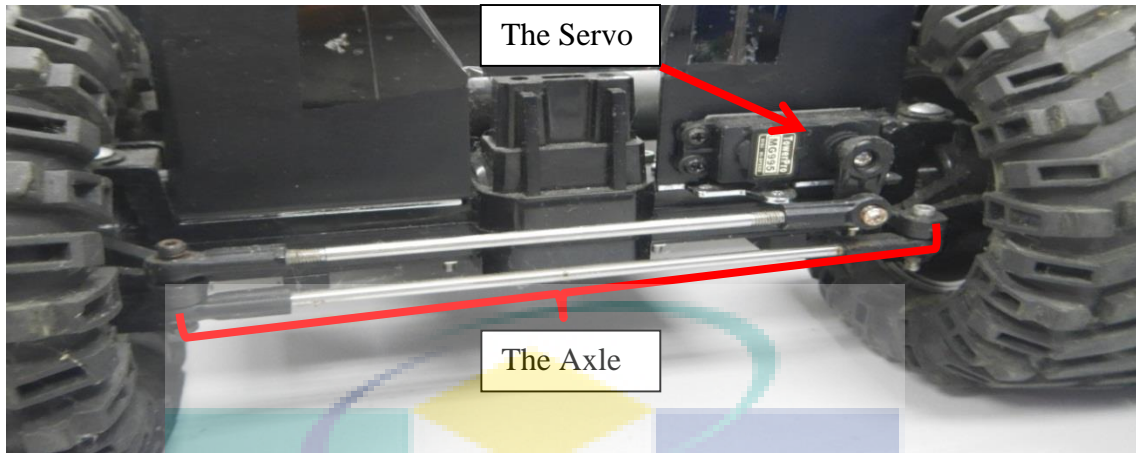


Figure 3.2: Front axle connected to the front servo.

At the front axle, the relationship between the wheel's front steering angle (α_f) and steering angle of the front left (γ_{fe}) and the front right (γ_{fg}) wheels can be derived as shown in equation 3.1 taking into account the width of the AGV ($w_e + w_g$) and β is the heading angle of the AGV. Equation 3.1 is only possible when the wheels at the same axle work in tandem with each other. Due to the symmetrical properties between the front axle and the rear axle, equation 3.1 also holds for the rear axle model wheel when α_f is substituted with α_r , γ_{fe} is substituted with γ_{re} , and γ_{fg} is substituted with γ_{rg} .

$$\alpha_f = \arctan \frac{(w_e + w_g)(\tan \gamma_{fe} \tan \gamma_{fg})}{(w_g \tan \gamma_{fg} + w_e \tan \gamma_{fe})} \quad (3.1)$$

Since the wheels work in pairs at the front axle and rear axle, the sketch in figure 3.1 can further be simplified by introducing a two wheels model at the intersection point of the AGV longitudinal axis and the front and rear axle as shown in figure 4.3. This model is usually called the bicycle model where the simplified body movement is controlled by a wheel at each end of longitudinal axis of the body. Since the AGV uses two DC motors to drive the front and the rear wheels, the bicycle model is considered an appropriate adaptation.

From figure 3.3, v is the AGV's velocity with reference to its CoG, and δ is the angle from the AGV longitudinal axis to vehicle's velocity. The angle δ is known as the side-slip angle. The side-slip angle allows translational movement to either side without

having to rotate. Meanwhile, β is the heading angle of the AGV. It is measured from the X-axis to the vehicle longitudinal axis.

The velocity, side-slip angle, and heading angle are derivatives from the motors driving the wheels at each axle. Since the motors run independently from each other, the front wheel velocity, v_f and the rear wheel velocity, v_r , have to be defined. Referring to figure 3.1, it can be seen that the model wheel is at the intersection of the longitudinal axis and the front axle and the rear axle respectively, thus defining the location of the wheel's driving velocity.

Likewise, the steering angle for both, the front wheels, α_f and the rear wheel, α_r , are also defined at the same location where the angle is the rotational deviation of the wheels from the AGV's longitudinal axis l_f and l_r then is defined as the length between the CoG of the AGV to the front and rear axle respectively. Comparing figures 3.1 and 3.3, that the angle α_f and the angle α_r describing the same angle properties in both figures. Thus, it shows the bicycle model is a suitable model for the four wheels AGV.

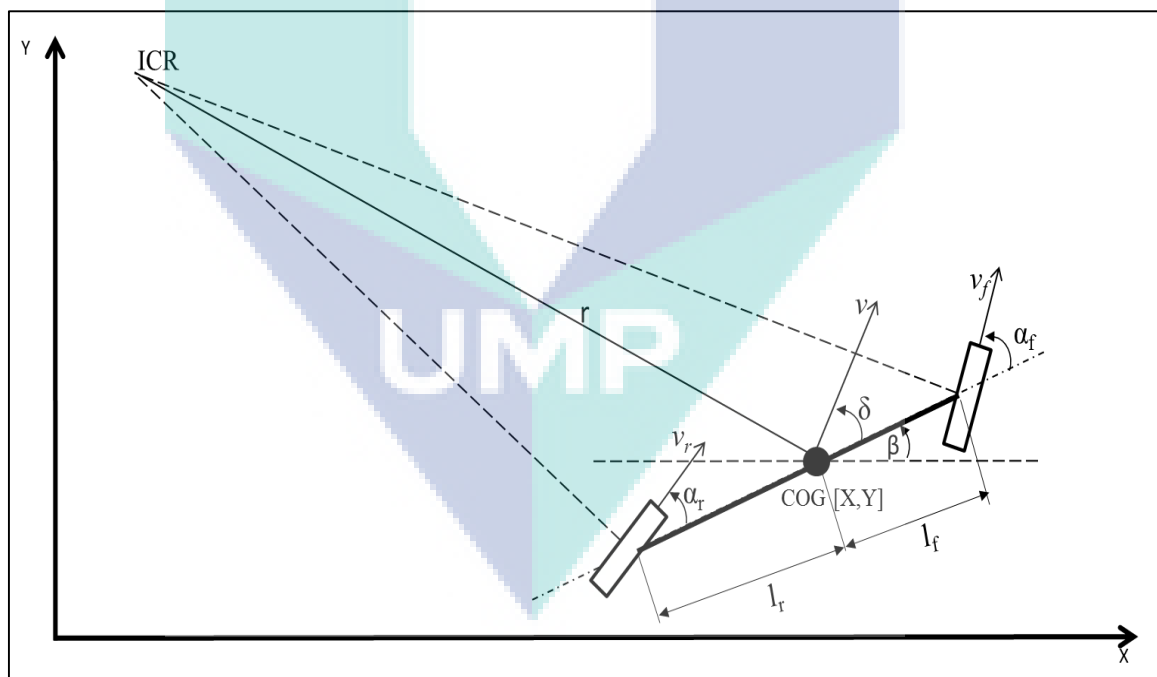


Figure 3.3: Bicycle model of the AGV.

As the AGV moves in the global coordinate system, its movement can be calculated by using rate of change horizontal distance (\dot{X}), rate of change vertical distance (\dot{Y}) and the rate of change heading angle ($\dot{\beta}$). With the necessary terms explained, the kinematics model of the vehicle can be expressed by equation 3.2, 3.3, and 3.4:

$$\dot{X} = v \cos(\beta - \delta) \quad (3.2)$$

$$\dot{Y} = v \sin(\beta - \delta) \quad (3.3)$$

$$\dot{\beta} = \frac{v \cos \delta (\tan \alpha_f - \tan \alpha_r)}{l_f + l_r} \quad (3.4)$$

where

$$\delta = \arctan \frac{l_r \tan \alpha_f + l_f \tan \alpha_r}{l_f + l_r} \quad (3.5)$$

$$v^2 = \frac{v_f^2 + v_r^2 + 2v_f v_r \cos(\alpha_f - \alpha_r)}{4} \quad (3.6)$$

It should also be noted that the wheel velocities magnitudes and steering angles are derived from the magnitude and the compound angle of the left and right wheels from the same axle. Therefore, the input variables for this model are v_f velocity at the front wheel, v_r velocity at the rear wheel, α_f turning angle of the front wheel, and α_r turning angle of the rear wheel.

Due to mechanical constraint, the steering angle can only vary within a certain range. Therefore the minimum turning radius must be determined. The minimum turning radius divides the global coordinate area into two regions. The area inside the minimum turning radius cannot be reached by the AGV from its current position. From equation 3.4, the turning radius can be derived from the angular speed equation ($v = r \cdot \omega$). Thus, the radius is given by:

$$r = \left| \frac{l_f + l_r}{\cos \delta (\tan \alpha_f - \tan \alpha_r)} \right| \quad (3.7)$$

One of the advantages having four wheels steering is zero-side-slip manoeuvre (Danwei and Feng, 2001, Solea et al., 2010). Zero-side-slip manoeuvre is a vehicle manoeuvre situation when the direction of the vehicle velocity at the CoG always remains parallel to the vehicle longitudinal axis. This characteristic can be achieved by setting the side slip angle (δ) to zero. The side slip angle is given by equation 3.5. When navigating a curved path, the AGV's longitudinal axis with zero side slip will remain tangent to the desired path. This manoeuvre reduces the chance of the AGV straying from a desired curved path as the heading angle also remains tangent to the curve path.

Given that l_f is equal to l_r , as well as w_e equals to w_g , the AGV velocity will remain parallel to the AGV longitudinal axis when α_r is equal to negative α_f . As the front and the rear speed also can be set to be equal and renamed v_t , equation 3.6 can then be reduced to equation 3.8 with v_t and α being the revised input values.

$$v = \sqrt{\frac{v_t^2(1 + \cos 2\alpha)}{2}} \quad (3.8)$$

3.2 MOVING TO A POSE

Previously the mathematical representation of the AGV used in this research is presented. In this section the mathematical model of the AGV is used to move the AGV from a specific pose to another specific pose in the global coordinates.

3.2.1 Non-Holonomic Constraint

A holonomic robot is a robotic system that has equal numbers of actuation and degree of freedom. Since the AGV in this research has only two actuators, driving motor to move in the longitudinal direction and a servo motor to change the direction to the sides, but has three degrees of freedom as shown in equations 3.2, 3.3, and 3.4, the AGV in this research is a non-holonomic robot. Being non-holonomic, the AGV is subjected to a non-holonomic constraint (Jung-Min and Jong-Hwan, 1999, Dongkyoung, 2004). The non-holonomic constraint can be described in equation 3.9 when the AGV's tyres experience pure rolling without slipping.

$$\dot{Y} \cos \beta - \dot{X} \sin \beta = 0 \quad (3.9)$$

3.2.2 Position and Orientation

In the global coordinates, the AGV whereabouts can be tracked by locating the position with respect to the origin $[x, y]$ and the orientation of the AGV from the X-axis to its longitudinal axis $[\beta]$ as shown in figure 3.4. The coordinate $[X_1, Y_1, \beta_1]$ is the current pose of the AGV and the coordinate $[X_2, Y_2, \beta_2]$ is the desired pose of the AGV. The difference between current and final poses of the AGV can also be expressed in polar coordinates where ρ is the shortest distance between the AGV and the landmark and τ is the angle between the landmark, AGV and the x-coordinate.

$$\rho = \sqrt{(X_2 - X_1)^2 + (Y_2 - Y_1)^2} \quad (3.10)$$

$$\tau = \arctan\left(\frac{Y_2 - Y_1}{X_2 - X_1}\right) \quad (3.11)$$

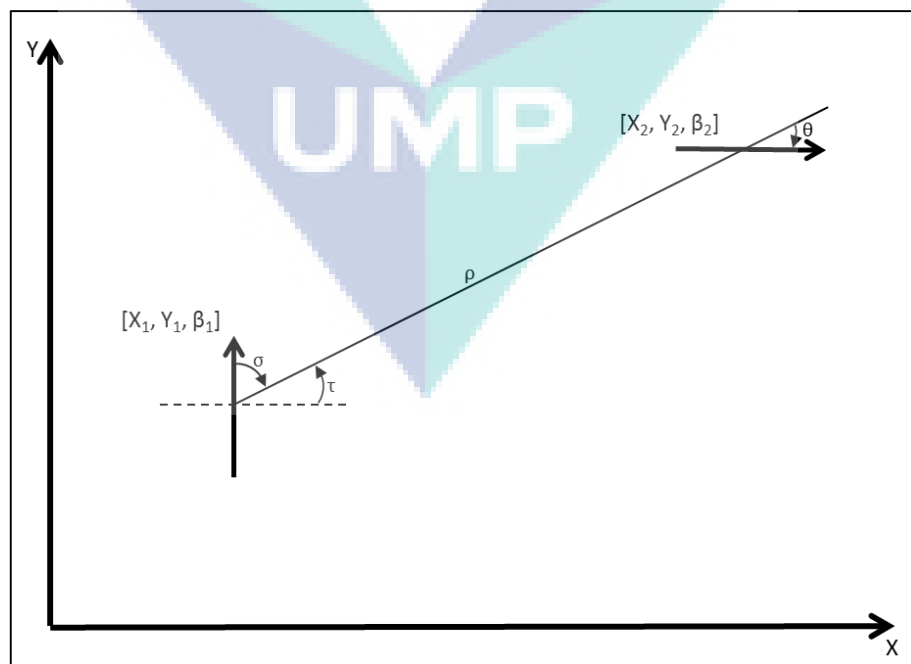


Figure 3.4: AGV in a global coordinates

Another two important angles to be determined are: σ , which is measured from the AGV longitudinal axis and ρ , and θ , which is measured from ρ to the AGV longitudinal axis at the final pose. The term ρ and σ drive the AGV toward the final position and the term θ rotates the AGV towards its final orientation.

$$\sigma = \tau - \beta \quad (3.12)$$

$$\theta = -\beta - \sigma \quad (3.13)$$

3.3 MOVING WITH CAMERA PERSPECTIVE.

The AGV used in this research employs an omnidirectional camera as the range sensor for tracking its movement within a space. As a sole sensor on board the AGV, the camera has several tasks to perform simultaneously. The main task is to locate and detect the nearest landmark relative to its current position. Apart from that, the camera must determine the relative position and orientation of the AGV to the global coordinates. As the AGV moves, the camera also moves. Therefore, this section describes how the omnidirectional camera is used to measure several critical values in order to function as a range sensor for the AGV.

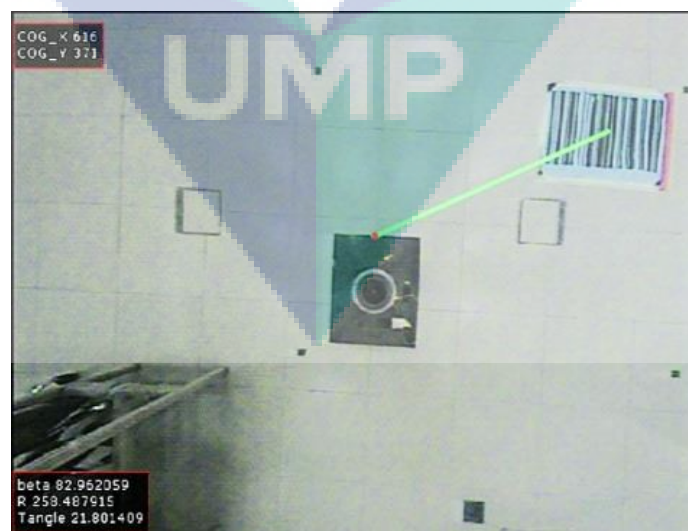


Figure 3.5: On-board omnidirectional camera view

An image captured by the omnidirectional camera is shown in figure 3.5. In this image, two distinct features can be seen namely, the landmark and the AGV. From the landmark feature, the CoG of the landmark is marked by a point. The point then represents the current x and y coordinates of the landmark in the image from the camera coordinate system.

Since the landmark's pose is known in the global position, the landmark is a key component in the frame transformation from the global coordinate system to the camera frame coordinate system. The landmark, a blue barcode with a red strip on the right, when placed in a global coordinate frame, must take into account its position and orientation. The orientation of the landmark is given by the perpendicular axis of the landmarks red strip in terms of the global orientation β .

The camera coordinate system is fixed to the AGV's local coordinate system where as the AGV moves, the camera local coordinate system remains the same as the AGV local coordinate system. However since the algorithm allows the AGV to move relative to a fixed landmark, the position of the AGV in the global coordinates system can be ignored while the AGV is in motion. The camera system can measure the relative distance, ρ , from AGV to the landmark and also the relative angle, τ_c , from the AGV to the landmark.

Nevertheless, in order to transform the AGV local orientation to the known landmark's global orientation, an angle between the x-axis of the AGV local coordinate and the red strip of the landmark, γ , is measured. The relationship between the global coordinates system and the AGV local system is given by the equation 3.15 where β_1 is the orientation of the AGV in global coordinate system and β_2 is the orientation of the landmark in global coordinate system.

$$\begin{aligned} \beta_1 &= \beta_2 - \gamma \text{ if } \beta_2 - \beta_1 > 0 \\ \beta_1 &= 180 - \gamma + \beta_2 \text{ if } \beta_2 - \beta_1 < 0 \end{aligned} \quad (3.15)$$

However, the relative angle, τ_c , from AGV to the landmark measured by the camera is not the τ presented in equations 3.11 and 3.12. In order to calculate τ from camera measurement, a transformation angle (T_a) between the local coordinate system and the global coordinate system must be determined. The AGV will only rotate about the z-axis in relation to the global coordinate system and the x-axis and the y-axis of the

global coordinate system, as well as the x-axis and the y-axis of the image remain at 90° to each other throughout the movement. The transformation angle is given by equation 3.16. Thus from the calculated transformation angle, τ can be calculated from equation 3.17:

$$T_a = 90 - \beta_1 \quad (3.16)$$

$$\tau = \tau_c - T_a \quad (3.17)$$

3.4 CONTROLLING THE AGV MOVEMENT

The AGV movement is controlled by the difference of the current position and orientation (pose) from the target pose. The target pose is given by the landmark's pose and the current pose of the AGV relative to the landmark is detected by the omnidirectional camera. Figure 3.6 shows a simplified block diagram for the feedback control of the AGV.

The AGV is designed to slow down as it is nearing the target. Therefore, based on the position input from the controller the AGV on board computer calculated the necessary PWM signal required to power the motor speed.

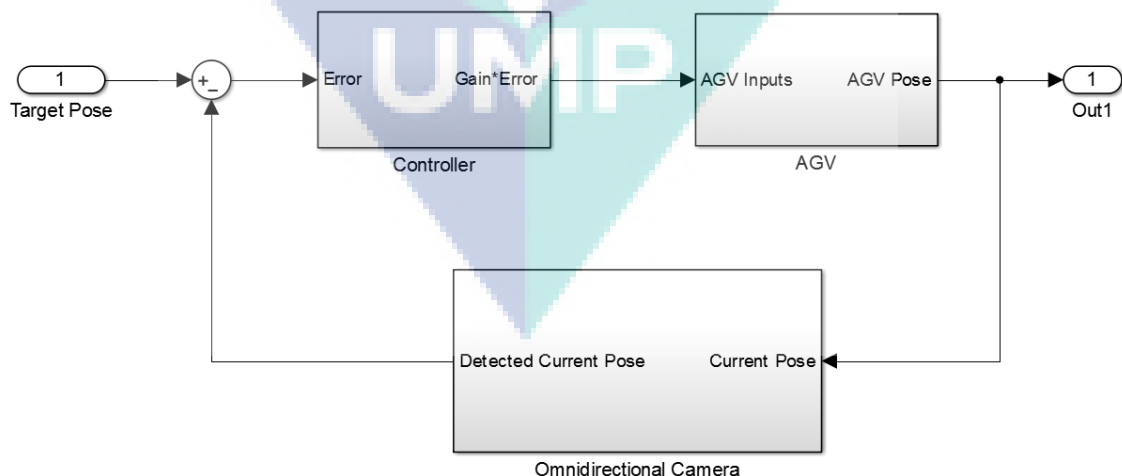


Figure 3.6 : Simplified Block diagram for the feedback control of the AGV

The position of the AGV is determined by X-coordinate and Y-coordinate in a global coordinate system. This position is constantly tracked by the omnidirectional camera on board the AGV. The difference between the target position and the current position is used to apply proportional control for the AGV. Equation 3.18 and 3.19 show the controller equation for position used where TP is the target position, CP is the AGV's current position and K_p is the proportional gain for both position components. The subscript shows the coordinate components.

$$X^* = K_p(TP_x - CP_x) \quad (3.18)$$

$$Y^* = K_p(TP_y - CP_y) \quad (3.19)$$

The orientation of the AGV is governed by σ and θ where the term σ drive the AGV towards the target and the term θ . Both terms are dependent on the difference of target orientation and current orientation. Equation 3.20 and 3.21 show the controller equation for orientation used where TO_β is the target orientation, CO_β is the AGV's current orientation and K_σ and K_θ are the proportional gains. Figure 3.7 shows the MATLAB/Simulink block diagram for the AGV controller.

$$\sigma^* = K_\sigma(TO_\beta - CO_\beta) \quad (3.20)$$

$$\theta^* = K_\theta(TO_\beta - CO_\beta) \quad (3.21)$$

The tuning of the proportional gain is done by trial and error. The system is stable so long the following conditions are met:

$$\begin{aligned} K_p &> 0 \\ K_\sigma &< 0 \\ K_\theta - K_p &> 0 \end{aligned} \quad (3.22)$$

From simulation results, the system was proved to be asymptotically stable.

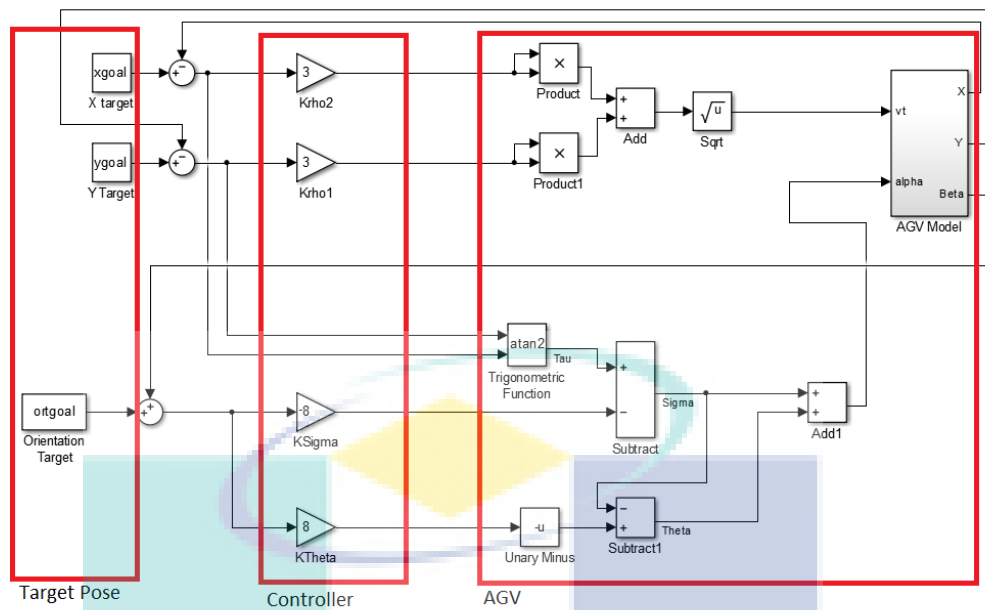


Figure 3.7 : MATLAB/Simulink block diagram for the AGV controller.

3.5 CHAPTER SUMMARY

This chapter presents the necessary equations needed in order to move the AGV to the landmark. These equations are then used to simulate the AGV using MATLAB and then realized through the image processing software and programming in the actual AGV. The comparison between the simulation and the experimental version will then be analysed for the third objective which is to generate the trajectory for the AGV to align and position itself with a landmark.

CHAPTER 4

RESEARCH METHODOLOGY: EXPERIMENTAL SETUP

4.0 INTRODUCTION

This chapter discussed the assembly phase and the setup for experimental works. The experimental works including identifying detecting and recognizing landmarks and the trajectory generation using image processing for the AGV's alignment with the landmark.

4.1 ASSEMBLY OF THE AGV WITH OMNIDIRECTIONAL CAMERA

The AGV platform used in this research has the following characteristics. The actuators for the vehicle are two DC motors and two servo motors. The sensor is an omnidirectional camera with wireless transmitter. Perception is completed by image processing in Roboreal software with a Bluetooth transmitter. Motion planning and control is executed through microcontroller programming.

4.1.1. The AGV platform.

The AGV was built on a 586 mm (L) x 470mm (W) x 158mm (H) mobile platform as shown in figure 4.1(a). Two motors were used to drive the wheels with a motor to turn both wheels at the front axle, shown in figure 4.1(b), and another motor at the rear axle. In order to steer the wheels, two servos are used, one servo for each axle shown in figure 4.1(c).

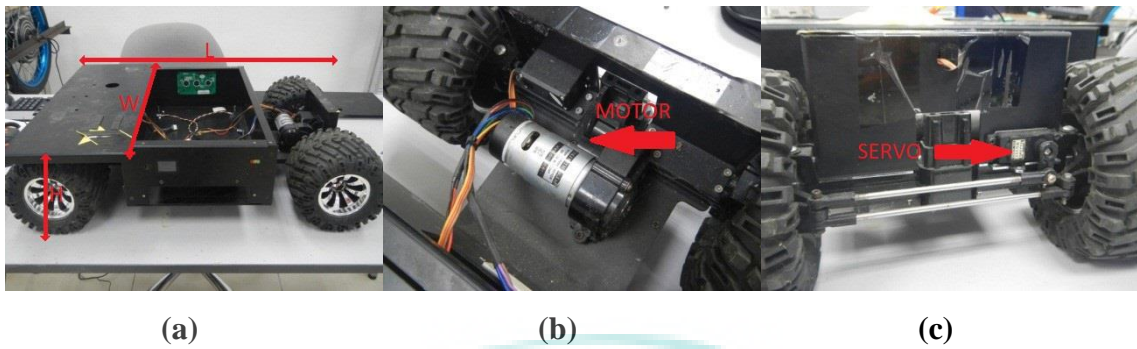


Figure 4.1: (a) The AGV dimensions (b) Front-axle motor (c) Servo motor for front axle.

4.1.2 The Omnidirectional Camera and Its Holder

The omnidirectional camera used in this research was a perspective camera with a conical mirror on the focal point of the camera as shown in figure 4.2. A cylindrical aluminium casing with outside diameter 32 cm protects the camera and a parabolic transparent plastic maintains the distance of the camera and the mirror. The objects from the environment were first reflected on the mirror before being focused into the camera. The camera has a resolution of 720 pixel x 480 pixel.

Since the AGV platform CoG is at the centre of the platform, the camera must be mounted also at the centre. This increased the height of the CoG from the floor but its position still remains at the centre. Besides, as the camera could capture image 360° of the horizontal plane, it is also logical to place the camera at the centre of the mobile platform. Furthermore, the higher the camera was placed, the wider the object area captured by the camera.

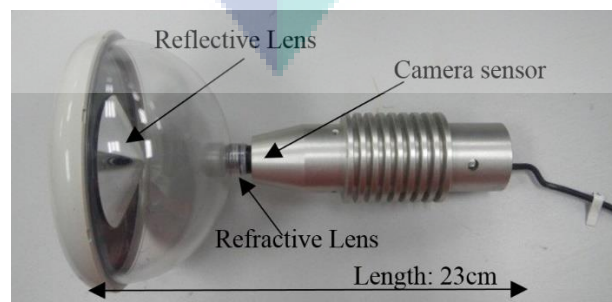


Figure 4.2: Omnidirectional camera used in this research.

A camera holder was therefore designed to accommodate the aforementioned features. The camera was placed on top of the mobile platform at the platform's CoG. The camera holder was produced using a rapid prototyping machine consisting of three segmented pieces which could be adjusted to the desired height with 10cm increment. The first segment of the camera holder was the base part. The base of the camera holder was bolted directly to the top of the platform. It was designed to hold the weight of the camera and its holder.

The second segment of the camera holder was the top part. The top segment was a cylindrical piece with 36 mm diameter and 100 mm length that holds the camera. The third segment was the middle part. This segment was also a cylindrical piece with 36mm diameter with 100mm connecting the base and the top segment. The middle segment was duplicated two times in order to have a total of 400mm height from the top of the platform to the bottom of the camera aluminium housing.

4.1.3 The Microcontroller and Communications

The microcontroller used to control the motor drive and the steering of the mobile platform is an open source electronics prototyping board, Arduino Uno. The board uses an ATmega328 microcontroller with 14 digital input/output (IO) pins and 6 analogue input pins. A two ampere motor driver shield from DFRobot was used to drive both motors using pulse width modulation (PWM) signals and another two PWM signals for controlling servo motor. In order to control the motion of the mobile platform, four PWM signals is needed where two signals for the two DC motors and 2 signals for the two servo motors. Thus, the microcontroller was programmed to receive these four PWM signals through Bluetooth communication after the image was processed by a workstation. Part of this program can be seen in figure 4.3 and the complete program can be seen in Appendix B.

```

if (MyString.length() >1)
{
  int n = MyString.toInt(); //convert MyString into a number
  Serial.println(n); //print value of n (index of character)
  if(MyString.indexOf('a') >0) myservoa.write(n);
  if(MyString.indexOf('b') >0) myservob.write(n);
  if(MyString.indexOf('z') >0) // Forward control index
  {
    digitalWrite(4,HIGH); //
    analogwrite(5, n);
    digitalWrite(7,HIGH); //
    analogwrite(6, n);
  }
  if(MyString.indexOf('y') >0) // Reverse control Index
  {
    digitalWrite(4,LOW);
    analogwrite(5, n);
    digitalWrite(7,LOW);
    analogwrite(6, n);
  }
}
MyString=""; //clears variable for new input

```

Figure 4.3 : Partial programming code for the AGV.

4.1.4 The Image Processing Software

The perception of the mobile robot was governed by the vision algorithm established through an image processing software called RoborealM. RoborealM is a commercially available software for image processing. The software processes an image through modular algorithms such as image morphology, image colour space, image thresholding, image filtering and image matching. The software also allows script plugin for control extension. At the end of the image processing stages, control signals can be sent to the mobile platform through a serial module with a Bluetooth communication port

The graphical user interface (GUI) of the RoborealM software is shown in figure 4.4. The main section of the GUI feature the video images captured from a camera. The left column of the interface shows the modules available for image processing, communications and some preloaded robotics control modules. The bottom row shows the modules selected by the user in order to execute the image processing.

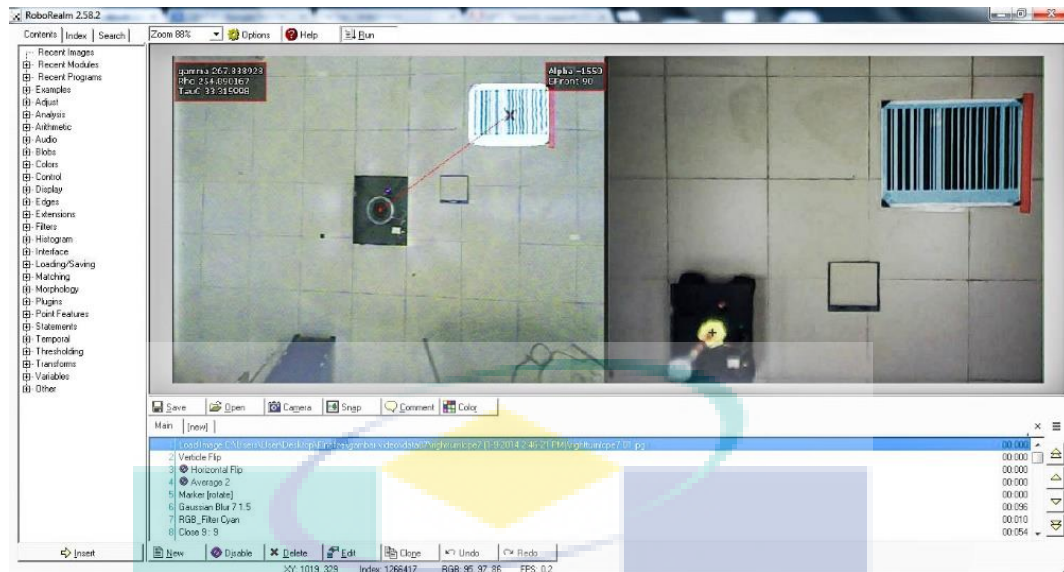


Figure 4.4: Roborealm GUI

4.1.5 The Assembly

Figure 4.5 shows the final assembly of the AGV. Towering 80 cm on top the AGV was the omnidirectional camera. A small box beside the tower houses the radio signal transmitter to transfer the image captured by the camera to the workstation. The AGV was powered by a 14.8 V Lithium Polymer battery and the camera and its transmitter were powered by an 11.1 V Lithium Polymer battery.

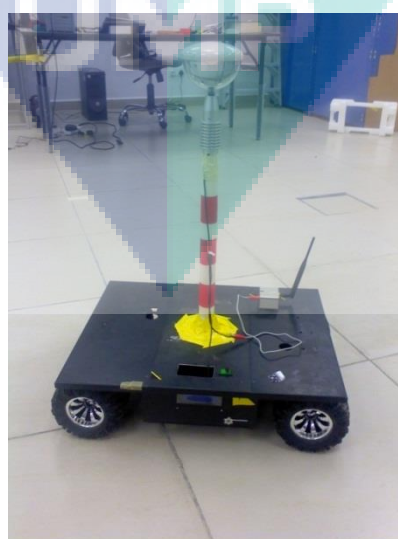


Figure 4.5: The final assembly of the AGV

4.1.6 The Side Slip Test

Before the AGV is operated in fully autonomous mode, a manual test control was conducted. This test is to ensure that the AGV behaves like the derived mathematical model of equations 3.2, 3.3, 3.4, 3.5 and 3.6. The test consists of a lane changing test with first a positive steering angle and then a negative steering angle whilst at a constant speed of 0.32 m/s. The AGV should then first turn to the left and then turn to the right thus mimicking a car changing lanes. The position of the AGV is tracked by an overhead camera. The result of this experiment is discussed in section 5.1. The speed 0.32 m/s was chosen due the area limitation of overhead camera to track the AGV. At faster speed the turn occurred outside the field of view of the tracking camera.

4.2 IDENTIFYING, DETECTING AND RECOGNIZING LANDMARKS FOR THE AGV USING OMNIDIRECTIONAL CAMERA.

In these experiments, the detectability of the landmarks was evaluated. Two main experiments were conducted for this purpose. First, a static detection experiment was conducted where the landmarks were detected while the AGV was fixed in one place. Second, in motion detection experiment was conducted where the landmarks were detected while the AGV was in motion.

4.2.1 The landmarks

The landmarks used must be salient and distinctive. The landmark chosen for this study was an enlarged Code-128 standard barcode. It can be changed to any barcode standard that suits the operation of the company as the standard barcode is widely used as machines tag for asset inventory. As the barcode is unique to the particular machine where it is tagged, the AGV could localize itself about the machine and performed the same task on the machine station even if the machine was moved due to layout changes. However, a little modification was required to the standard barcode to make it more salient to the background. The barcode used in this study includes a cyan background instead of a white background and bears a red strip on top for orientation as shown in figure 4.6. These landmarks were placed in specific known locations in the global coordinate perspective thus creating points of interest for the AGV to move to.



Figure 4.6: The barcode use in this study

4.2.2 Static detection experiment setup

The main objective of this experiment was to determine the suitable size of the barcode to be used as the landmarks. A set of barcodes are printed on A4, A3, A2, and A1 size papers shown in figure 4.7. Then the barcodes were placed either on the side of the AGV or on the front of the AGV. The barcodes were also placed standing up figure 4.7(a) or laid flat on the floor shown in figure 4.8(b). The illumination for standing up barcodes was about 500 lux while for on the floor barcode was about 900 lux.

The image captured by the AGV is processed by the Roborealms software. The image went through a histogram levelling process before a barcode matching feature in Roborealms was used to decode the barcode. Since the encoded number in the barcode was known, a successful detection was recorded only when the software decode the same encoded number of the barcode. The result of this experiment was presented in the next chapter.

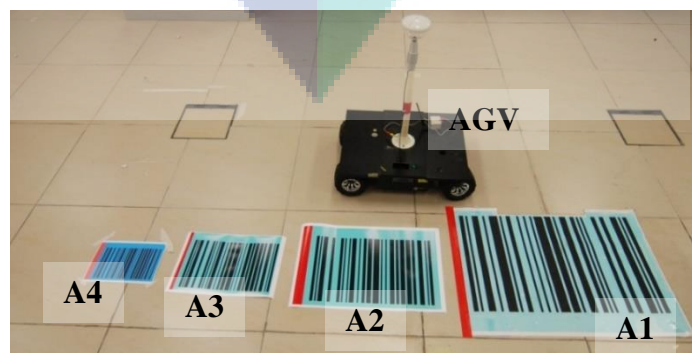


Figure 4.7: Sample of barcodes size tested in this experiments

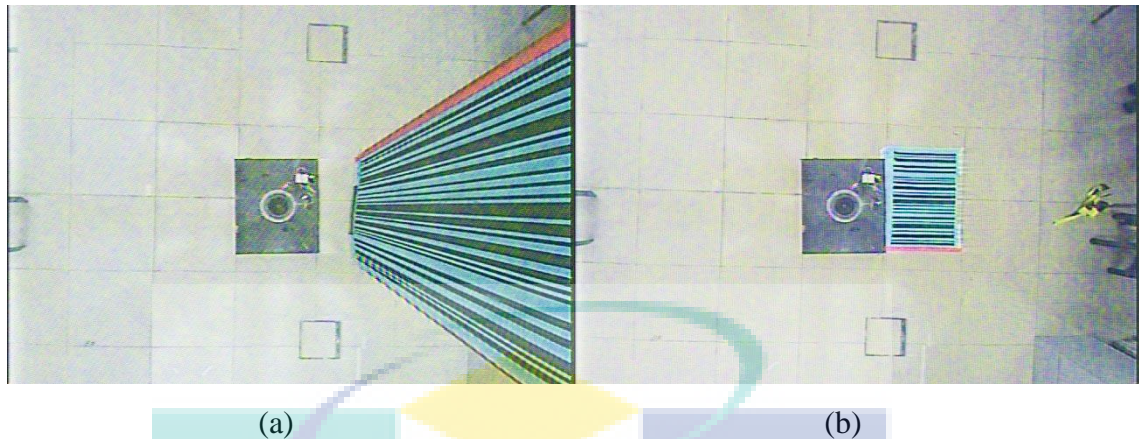


Figure 4.8: Position of the landmark standing up (a) and flat on the floor (b)

4.2.3 In-motion detection experiment setup

The main objective for the in motion detection experiment was to determine the suitable size of the barcode to be used as the landmarks while the camera was in motion. Similar to the static detection experiment, four sizes of barcodes were printed on A1, A2, A3, and A4 papers. Then the four different barcodes of the same size were placed standing up in a straight line. The illumination for the barcodes was about 500 lux. The AGV then, moves in a straight line to detect all four barcode while in motion. The speed of the AGV was set at 0.32 m/s. Four runs at the same speed was conducted to ensure the reliability of the detected barcodes.

Similar to the static detection experiment, the image captured by the AGV was also processed by the Roboreal software and went through the same process of histogram levelling and a barcode matching process. Successful detection was recorded only when the software decode the same encoded number of the barcode. The result of this experiments was presented in the next chapter.

4.3 TRAJECTORY GENERATION FOR ALIGNMENT WITH THE LANDMARK.

The main objective of this experiment was to investigate the path generated by the AGV microcontroller as compared to the path generated by the MATLAB simulation. In the MATLAB simulation several features were noted. First, the path was generated in the pixel scale of the tracking camera for the global coordinates system. Second, the orientation of the landmark was known initially. Third, the final position of the AGV was also known initially.

The experiments were conducted indoor with two cameras. The main camera was the omnidirectional camera on-board the AGV. Image processed from this camera governed the movement of the AGV. However, this camera can only track the position of the AGV in relation to the local coordinate system. Thus, a second camera was needed to track the AGV's position in global coordinate system. The second camera was a perspective camera placed on the ceiling about 3500 mm height from the floor. Figure 4.9 shows a picture of the experimental setup.

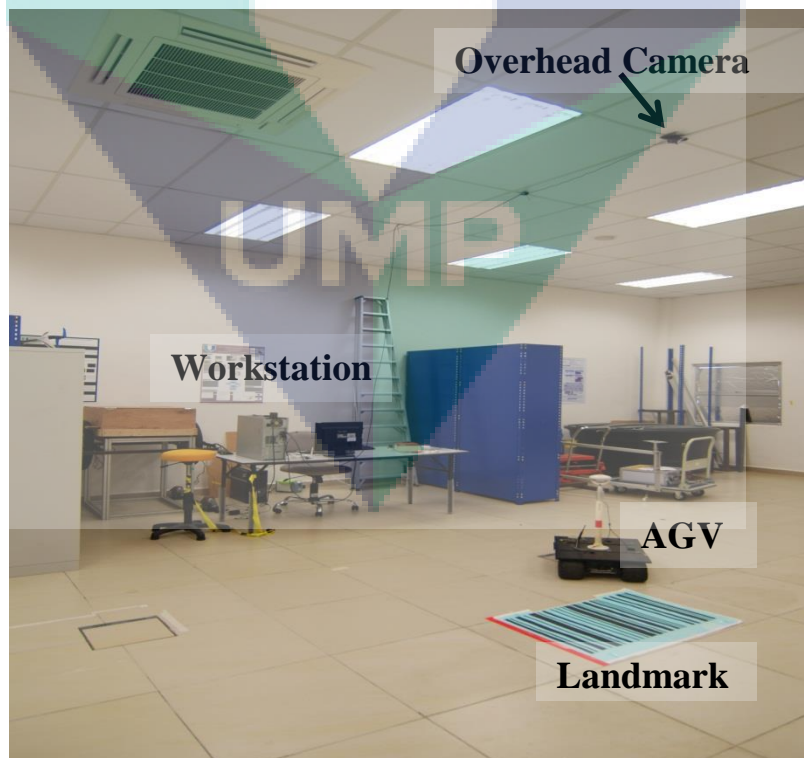


Figure 4.9: Experimental setup for trajectory test.

4.3.1 Image to object mapping.

Image mapping is a description of how the image captured by the camera correlates to the real world object. The image is usually measured in pixel unit while the real object in cm. In this research, the distance of the AGV and the landmarks in the x-y plane is very important. Therefore, an image mapping could help estimate the real distance.

The AGV was fixed to a position and a real distance centre of the AGV was measured horizontally and vertically in the x-y plane as shown in figure 4.10. Distances of 50 cm, 100 cm and 150 cm were marked on the floor. The image pixels from the camera centre to the marked distance were measured and the ratio was calculated. The result of the measurement is presented in Table 4.1. From the result, a 10 pixel image was mapped to a distance of 6.1 cm horizontally and 7.6 cm vertically.



Figure 4.10: Image to object mapping test on omnidirectional camera

Table 4.1: Result of image mapping by ratio method on the omnidirectional camera.

Horizontal		Vertical	
Real distance (cm)	Image distance (pixel)	Real distance (cm)	Image distance (pixel)
50	83	50	68
100	160	100	131
150	243	150	196

The second camera was a perspective camera. In order to map images to the object, an elaborate calculation can be made as shown by Taha and Jizat (Taha and Jizat, 2012). However, the second camera was always fixed in a specific position as opposed to the Taha and Jizat formulation. Therefore, a simple object to image ratio could mapped the whole image to the object.

A tile with measurement of 60 cm x 60 cm was used to determine the mapping. Horizontal and vertical pixel distances between the edges of the tiles image were measured. For both, horizontal and vertical distances, 150 pixels were measured. Thus every ten pixels captured by this camera gave an actual distance of 4 cm.

Images from both cameras, shown on figure 4.11, were processed by the same workstation to maintain synchronisation between the global and local coordinate systems.



(a)

(b)

Figure 4.11: Local (a) and global (b) view from the cameras

4.3.2 Image processing by RoborealM.

The image processing for the AGV was performed by the RoborealM software as mentioned in subsection 4.1.4. Images from the omnidirectional camera were received by the computer through a wireless AV transmitter. The image processing for the landmark detection and the AGV trajectory starts by denoising the images captured using the Gaussian blur module. The module makes the image blurry and at the same time reduces the noise level. However, blurring the image compromises the integrity of the barcode. The background colour of the barcode thus played an important role in detecting the landmark.

The images were converted into black and white by applying an RGB filter. The RGB filter isolates specific colour pixels (in this case cyan) and turned the pixel into a white mask and every other pixel into a black mask. The white mask was then dilated and eroded to joint all similar pixels to create a blanket of white mask over the landmark thus creating blobs of white mask.

Blob filter was then used to limit the blob into a specific size range of the landmark and any other blob discarded. The CoG of this blob then was determined to indicate the position of the landmark when viewed from the camera. The distance of the landmark CoG and the AGV's CoG was measured and the angle between the distance and the horizontal image line was determined. The measured distance represented as ρ in equation 3.10 and the measured angle represent τ_c used in equation 3.17.

The same process was repeated for the red strip on top of the landmarks. However, instead of determining the CoG of the red strip, the red strip was reduced to single pixel line skeleton. The angle between the skeletal line and the horizontal image line was then determined. This was the angle γ for equation 3.15. The image sequence of the image processing with the effect of each module to the image is shown in figure 4.12.

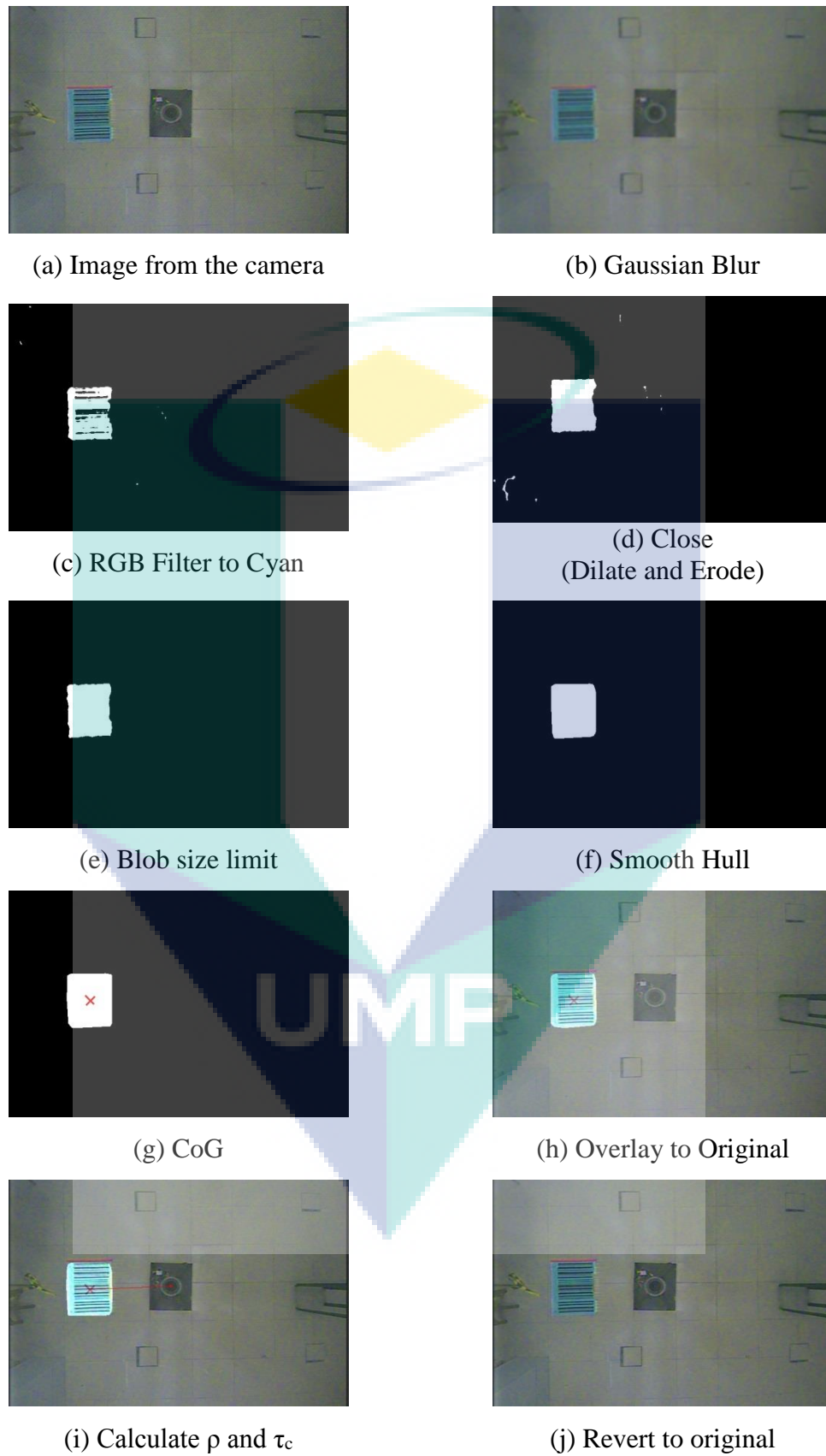


Figure 4.12: Image Sequences of the Image Processing and Its Effect to the Image

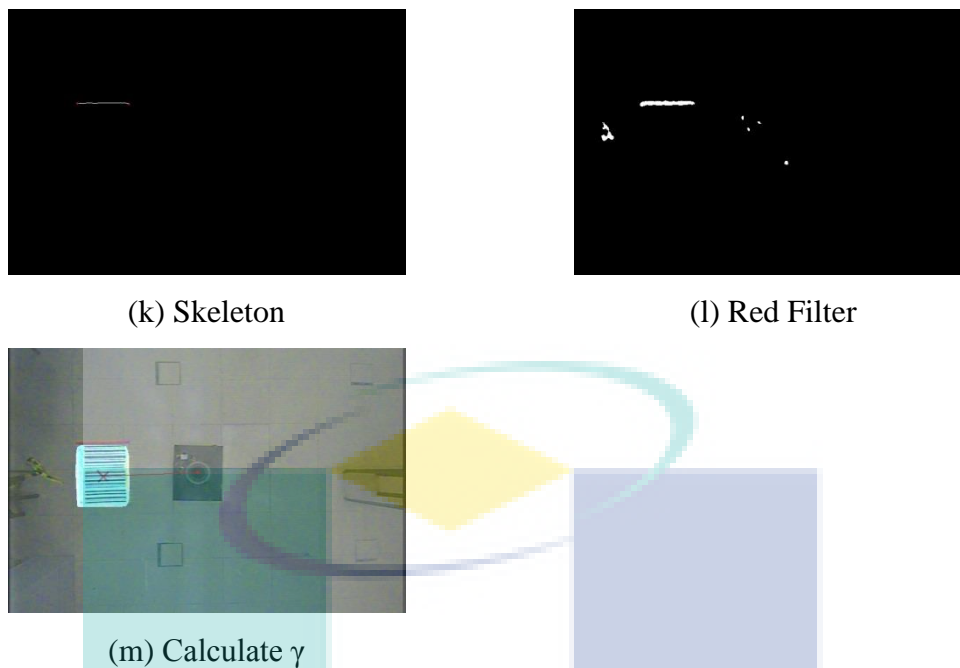


Figure 4.12: Continued

In order to track the position of the AGV, the same image algorithm was used on the second camera to track the yellow marker on the AGV. The yellow marker was placed at the bottom of the camera holder where the AGV's CoG was calculated. The images from both cameras were then combined using the Mosaic module, a module featured on the Roboreal software, shown in figure 4.13. The example of the combined image can be seen in figure 4.11. The position and orientation of the AGV for each motion were recorded and compared with the simulated position and orientation calculated from the MATLAB software.

All the equations governing the motion of the AGV were then programmed in Cscript module. The complete program instruction is shown in Appendix C. The outcome from this module was the four PWM signals mentioned in section 4.1.3. The four signals were sent through the Bluetooth serial by computer transmitter to the Bluetooth receiver on board the AGV. However, referring back to the equation 3.8, these four PWM signals were reduced to two signals where the front and rear speeds are at the same value and the rear steering angle is always negative of the front steering angle.

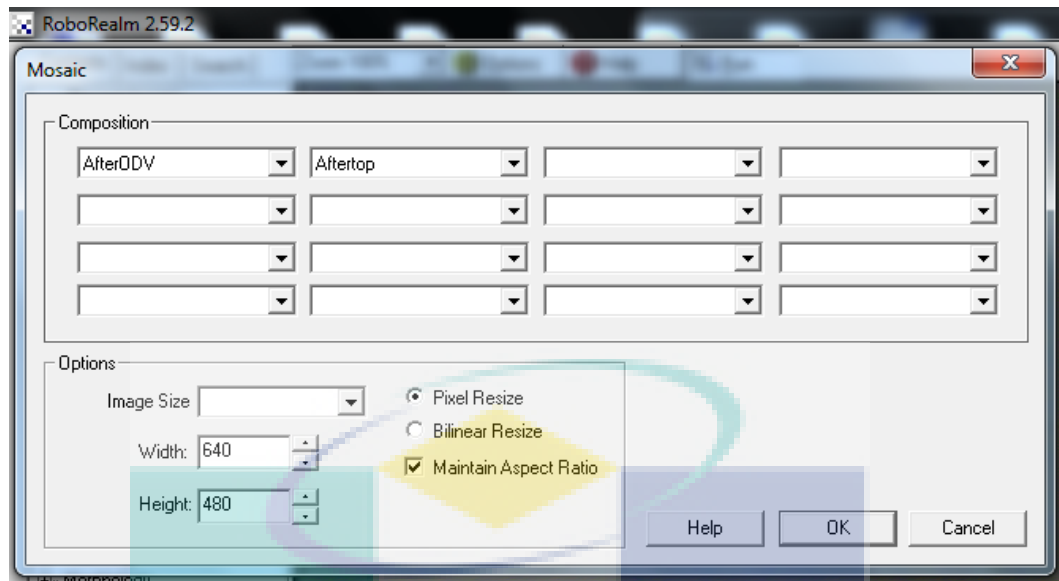


Figure 4.13: Mosaic Module User Interface

4.4 CHAPTER SUMMARY

Following the experimental setup for side-slip test, determination of the optimal size for landmark detection whilst stationary and in motion, and the AGV trajectory is described. These descriptions include mapping of the camera pixels of the on-board camera and the overhead camera to the actual distance and the algorithm for image processing.

UMP

CHAPTER 5

RESULT AND DISCUSSION

5.0 INTRODUCTION

In this chapter, the results from experiments on side slip test of the AGV, static and dynamic landmark detection, and comparison simulation of trajectory path in MATLAB/Simulink and experiments of trajectory path of the three forward movements are presented.

5.1 SIDE SLIP TEST OF AGV.

This section presents the result of the experiment conducted, as described in section 4.1.6. When given a constant speed input and positive and negative steering angle pulse input, the AGV then responds as if it was changing lanes. The simulation for this manoeuvre is shown by the blue colour line in figure 5.1. The same input was programmed in the CScript module of Roboreal software to physically manoeuvre the AGV. The position of the AGV was tracked by an overhead camera and compared to the simulation result. A constant speed of 0.3 m/s and 9° was given. When compared to the simulation results, the experimental result produced a similar manoeuvre as shown by the red line in figure 5.1.

The AGV was initially placed parallel to the horizontal line. After a moment a positive steering angle pulse was given. This made the AGV turned to the left from positions (100,100) to (350,200) as shown in figure 5.2. Then a negative steering angle pulse was given and the AGV made a right turn from position (350,200) onwards. The AGV maintained a forward straight line when there is no steering input. The input pulse for this is shown in figure 5.2.

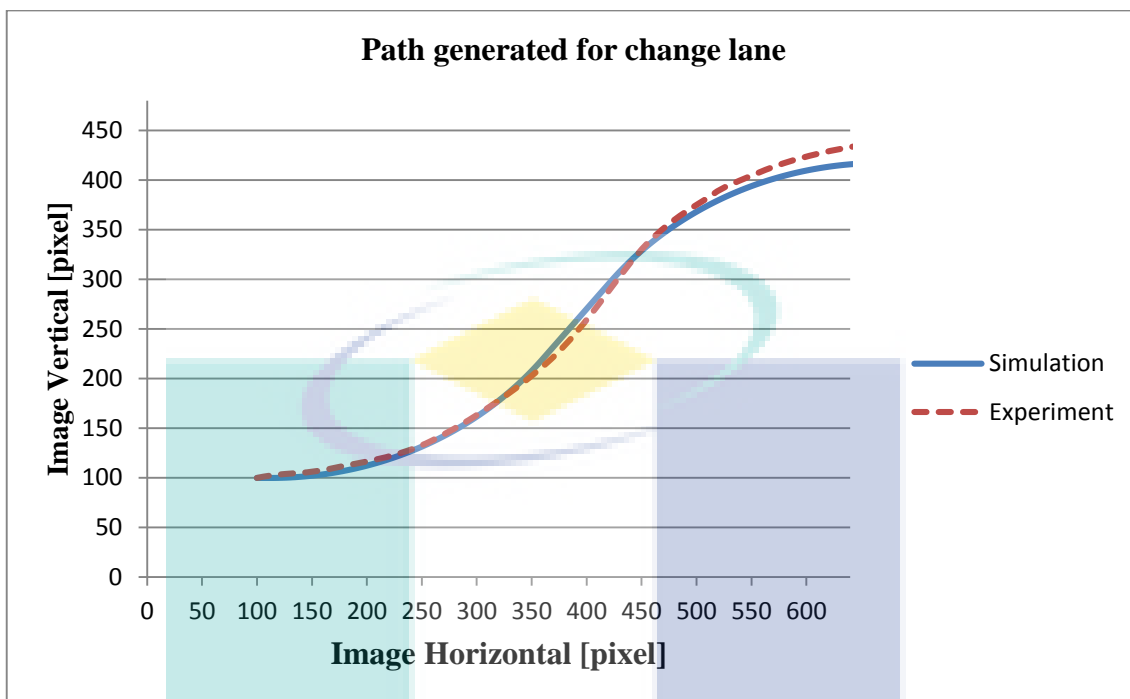


Figure 5.1: Comparison between simulation and experiment of direct input manoeuvre.

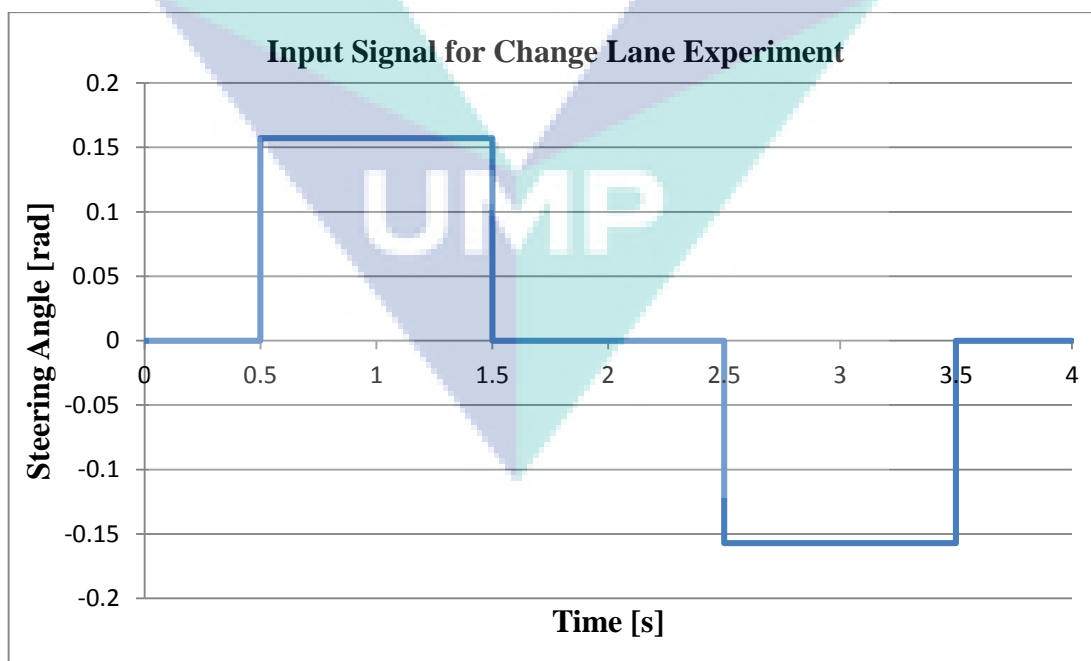


Figure 5.2: Input pulse for figure 5.1.

It should be noted that the AGV speed was relatively slow. If the speed was higher the greater curve generated would have caused the AGV to move outside the field of view of the overhead camera and its position could no longer be tracked.

The comparison between the experimented data and the simulation data showed the standard deviation of 11.0 pixels with the residual sum squares error of 1454 pixels². This standard deviation value is well inside 6 % margin of error where the tracked position consist of 480 pixel. The data calculations can be referred to Appendix A. However, the absolute data showed tendency of larger deviation at the end of tracked position compared to the initial position.

The equations which governs the residual sum square error and the standard deviation are shown in equation 5.1 and equation 5.3 respectively where RSE is the residual sum squares error, n is the number of data, $Yexp$ is the corresponding Y position at an X position gathered in the experiment, $Ysim$ is the corresponding Y position at an X position from the simulation work, VAR is the variance of the data and $STDEV$ is the standard deviation.

$$RSE = \sum_{i=1}^n (Yexp_i - Ysim_i)^2 \quad (5.1)$$

$$VAR = \frac{RSE}{n} \quad (5.2)$$

$$STDEV = \sqrt{VAR} \quad (5.3)$$

The steering angle, as it varies from zero to maximum left or right, will change the radius of curvature. The simulation result of the varying steering angle is shown in figure 5.3. The simulated values of the steering angle were 2°, 4°, 6°, and 8° and the duration of one second was maintained during the simulation. The smaller the angle the fewer curves the AGV will travel. This clearly shows that the turning radius play an important role in governing the AGV movement radius of curvature which is the reciprocal of the turning radius. If the AGV can turn at a larger angle, the AGV will become more agile. The input pulse for this is shown in figure 5.4.

It was also found that, as the angle varies from the zero to the maximum angle, the duration of the angle remained at a specific value can modify the path of the AGV. The simulation result of the varying the duration of steering angle and its input pulse is shown in figures 5.5 and 5.6 respectively. In the simulation, the steering angle was maintained at the 9° while the duration was varied from one second to 3 seconds. The AGV will travel along circumference of a circle if the steering angle remained at a specific angle long enough.

This side slip angle test showed that the steering angle can be controlled using PWM method in order to control the trajectory of the AGV. The similarity of the experiment and the simulation; less than 6 % error, showed that the AGV was well simulated by the bicycle model shown by equations 3.1 to 3.5 in chapter 3.

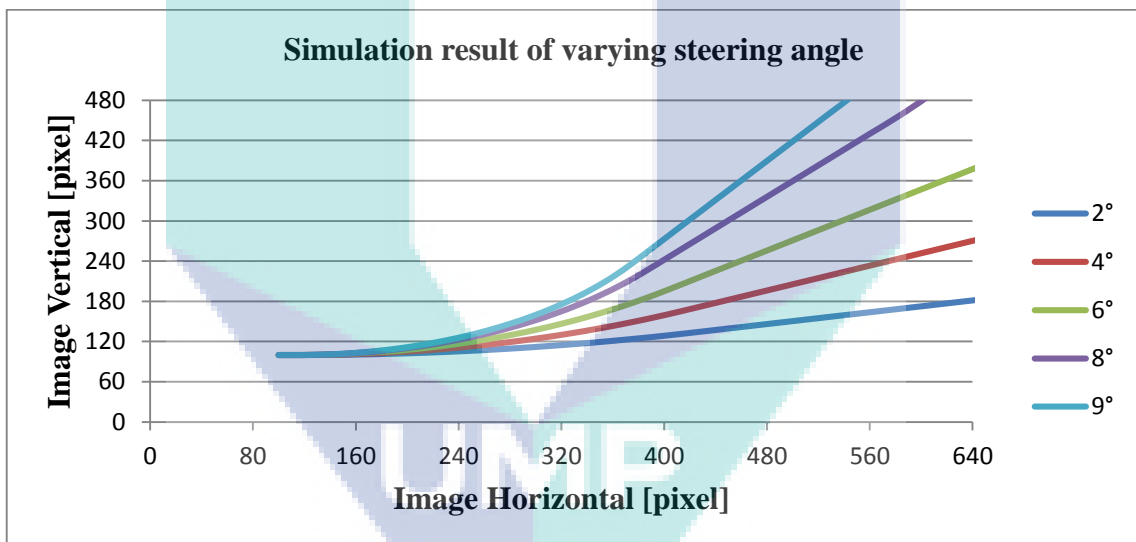


Figure 5.3: Simulation result of varying steering angle.

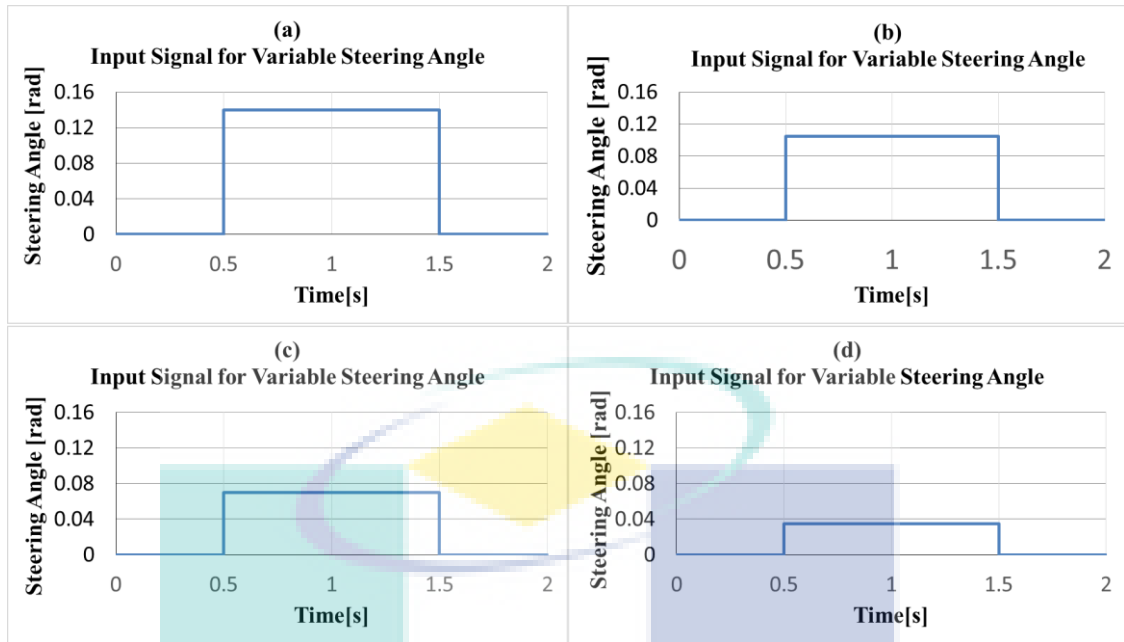


Figure 5.4: Input pulse for varying steering angle. (a) 8° left (b) 6° left (c) 4° left (d) 2° left.

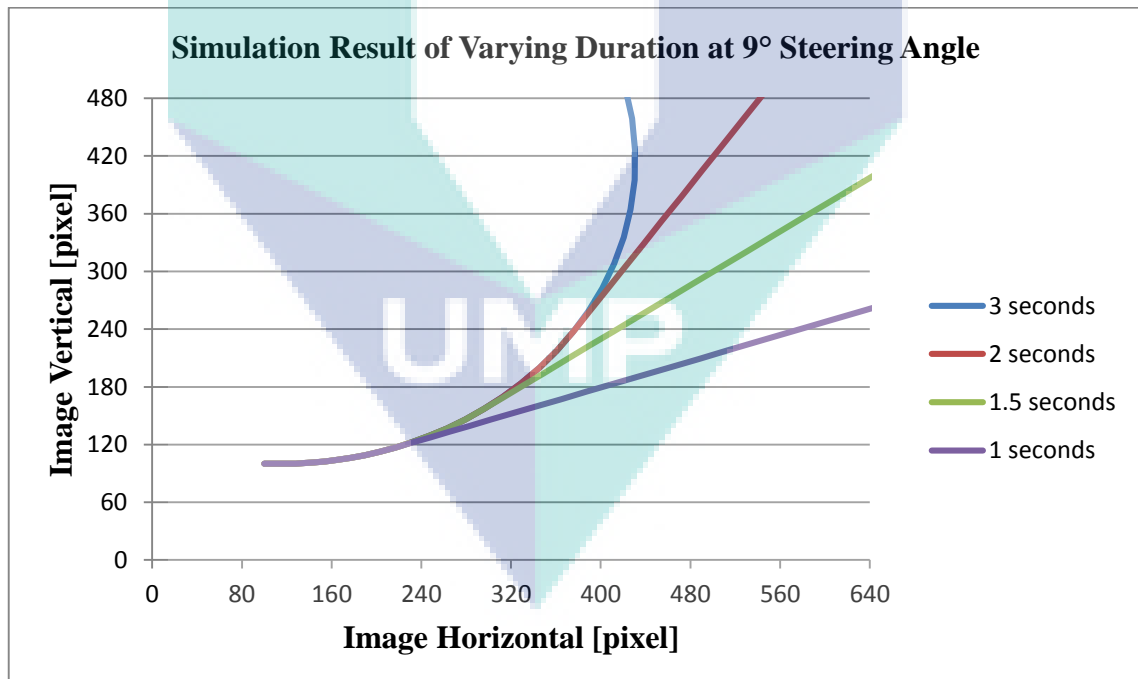


Figure 5.5: Simulation result of varying the duration of steering angle.

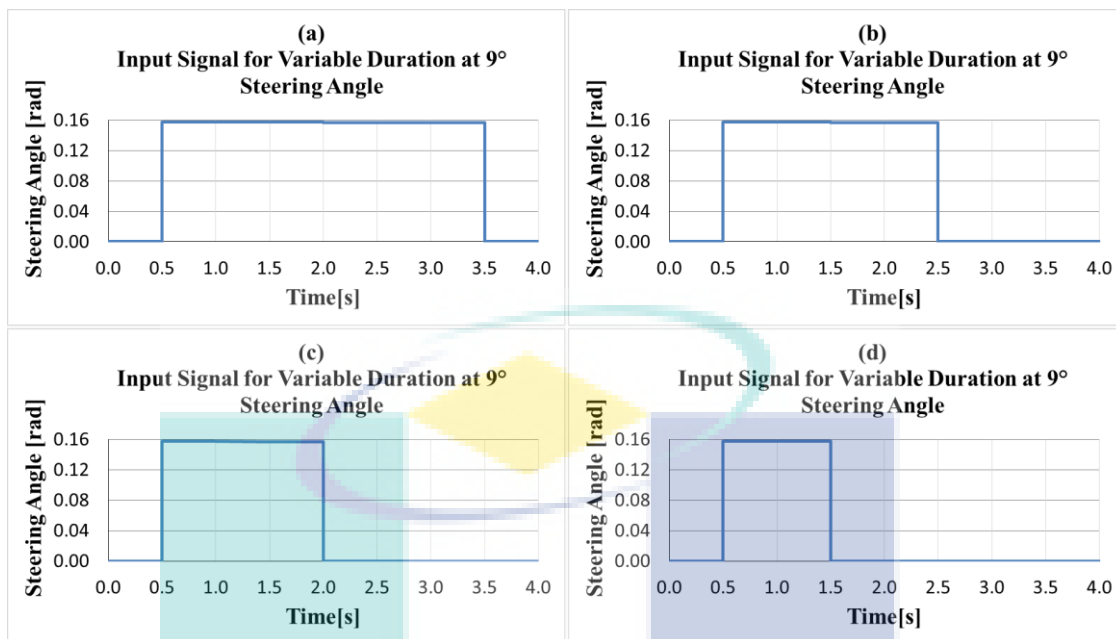


Figure 5.6: Input signal for variable duration of steering angle. a) 3 seconds, b) 2 seconds c) 1.5 seconds, d) 1 second.

5.2 LANDMARK DETECTION.

In this section, the results of the landmark detection experiments are presented. Two experiments were conducted in order to test the detectability of the landmarks. These experiments were mainly conducted to determine the ideal size of the landmark for detection. The experiments were conducted in two stages, first a static test, and second, in-motion test. Four sizes of the landmarks were tested. During the experiments, when the camera detected a correct landmark, a buzzer was activated.

5.2.1 Results of Static test

The results are tabulated in binary term whether the algorithm could detect the landmarks successfully or the algorithm failed to detect the landmarks. Table 5.1 shows the result of the first experiment where the landmarks is placed on the side of the AGV either standing up or laying down. The difference of the standing up and laying down setup is shown in figure 3.12 in chapter 3 using A1 size sample. Furthermore, the detected and recognized barcode generated a green line across the barcode as shown in figure 5.7

Table 5.1 shows that when the landmarks were placed on the side of the AGV, the smallest size of the barcode detected was the landmark printed on A3 size paper. The A3 size landmark could be detected even if the barcode is distorted when placed standing up. However, when placed at the front or rear of the AGV, shown in figure 5.8, only extra-large size barcode could be detected as shown in table 5.2.

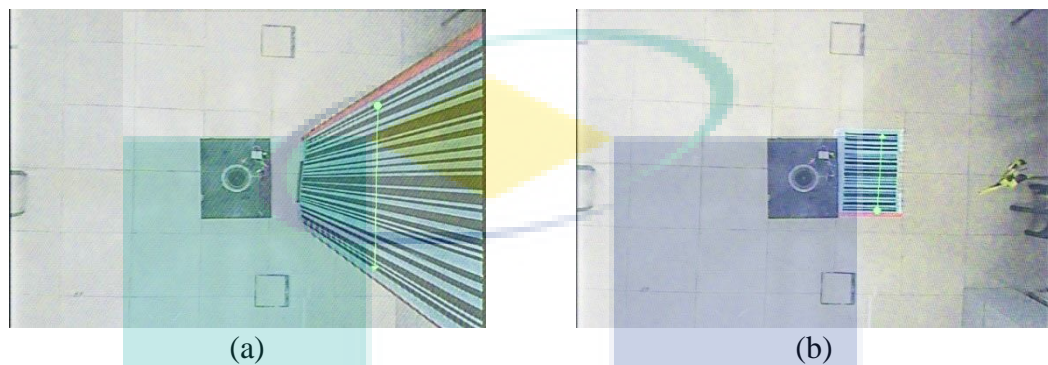


Figure 5.7: Detected and recognized barcode from the image. (a) Standing up barcode size A1. (b) Laying down barcode size A1.



Figure 5.8: (a) Barcode size A1 place in front of the AGV. (b) Barcode size A1 place on the side of the AGV.

Table 5.1: Result of experiments for with barcodes placed on the side of AGV.

Barcode size	Standing Up	Laying down
A4(small)	Not detected	Not detected
A3(medium)	Detected	Detected
A2(large)	Detected	Detected
A1(extra-large)	Detected	Detected

Table 5.2: Result of experiments for landmark placement on AGV's front or rear.

Barcode size	Standing Up	Laying down
A4(small)	Not detected	Not detected
A3(medium)	Not detected	Not detected
A2(large)	Not detected	Not detected
A1(extra-large)	Detected	Detected

From these two experiments, it is concluded that the extra-large barcode is ideal for detection with the omnidirectional camera's 720 x 480 resolution. The extra-large, A1 size, barcode had a greater area for mapping into image pixels compared to large, medium and small size barcodes. Thus, even if the image suffers from noise, the landmarks can be successfully detected.

The difference between the front or rear and side barcode placement is the detection area. The front or rear detection area is clearly smaller than on the side. When only the extra-large barcode was detected, it shows that the landmark size is affected by the camera resolution. A smaller camera resolution requires a larger landmark size.

5.2.2 In-motion experiment.

The In-motion experiment deals with landmarks detection while the AGV is in motion. Table 5.3 shows the results of the experiment when the AGV is moving at 0.3 m/s. The AGV in motion should detect four landmarks successfully in a row for each run. Four runs were conducted for each landmark size with the same speed. The multiple run was to ensure reliable result for landmark detection. At higher speeds than 0.3 m/s, the AGV could not detect any of the landmark size tested.

The results indicated that in order for successful detection, the AGV must travel at a speed no higher than 0.3 m/s when approaching the landmarks otherwise no landmarks can be detected successfully. In addition, only the A1 size landmark is detected consistently at this speed.

This result may be explained by looking at the deterioration of the landmark by size. Even in a static picture, shown in figure 5.9, the landmark is harder to be recognized

as the size of the landmarks shrink from size A1 to size A4. The deterioration becomes more severe as the AGV starts moving. As the camera was on board the AGV and was moving relative to a static landmark; the action created motion blur imagery of the landmark thus further deteriorating the image quality of the landmarks.

Table 5.3: Results for landmark detection while AGV is in motion

Landmarks size	Score			
	Run no 1	Run no 2	Run no3	Run no 4
A4	0/4	0/4	0/4	0/4
A3	0/4	1/4	0/4	1/4
A2	3/4	2/4	3/4	4/4
A1	4/4	4/4	4/4	4/4

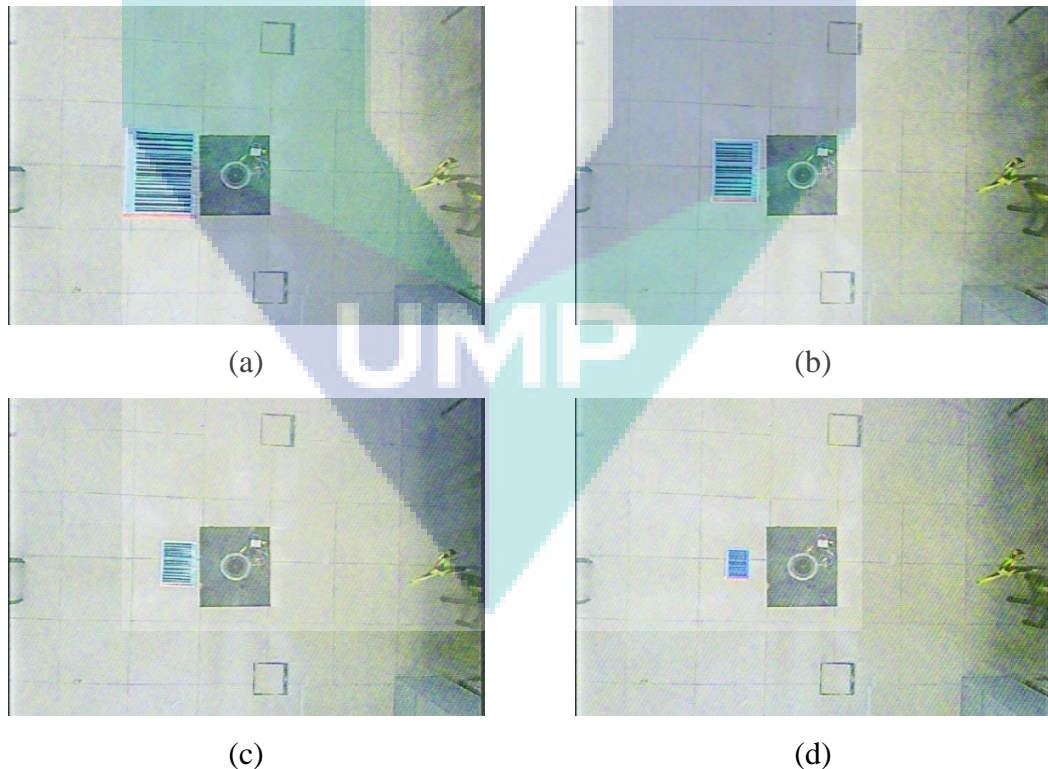


Figure 5.9: Comparison of the image barcode quality in static mode: (a) A1 size (b) A2 size (c) A3 size (d) A4 size

The landmarks used in this research are standard barcode code 128 with a colour background and a colour strip at the end of the barcode. The colour for the background and the strip improves the detectability and recognition of the orientation. It improves the saliency of the landmarks against wall or the floor paint. The specific colour is easily identified through colour filters or different colour space such as Hue-Saturation-Intensity. Coloured landmarks had been successfully experimented by Zhang et al. and Guanghai and Zhijian (Guanghai and Zhijian, 2011, Zhang et al., 2012).

The orientation of the landmark is important as the omnidirectional camera could detect the landmarks from any direction. By recognizing the landmark orientation, the vision algorithm could orient the AGV relative to the landmarks. Knowledge of the orientation is vital for navigation especially when the AGV is required to align itself to the landmark.

As highlighted by Briggs et al and Fiala, the standard barcode may have small gap between the bars detected by the camera (Briggs et al., 2000, Fiala, 2004). These small gaps between bars did presented a problem. However, with an appropriate camera resolution the problem can be resolved.

A1 size landmarks may not be practical for industrial usage. However, with the use of higher resolution cameras, smaller barcode landmarks can be used. This will lead to the application of 2D barcodes for navigation landmarks.

The experimental result shows that 1D barcodes can be successfully detected and read using omnidirectional camera without correcting the image distortion. The large size of the barcodes improves its detection using low resolution camera. Ideally, the AGV should be static while reading the barcode but the barcode also can be read while in motion at maximum speed of 0.3 m/s.

5.3 TRAJECTORY PATH EXPERIMENT

This section presents the result from trajectory simulation and trajectory experiment. The trajectory simulation was conducted using MATLAB. There were three trajectories experimented in this research, first, a trajectory when the landmark orientation was at 0° in front of the AGV, second, a trajectory when the landmark orientation was at 90° on the right of the AGV, and the third, a trajectory when the landmark orientation was at 90° on the left of the AGV. These three experiments represent the basic movements in AGV navigation namely straight line, right turn and left turn.

5.3.1 Straight trajectory

In this experiment, the starting pose of the AGV was (76, 315, 0) and the landmark was positioned at (500, 350, 0) in pixel coordinates with reference to the global coordinates system. The landmark used in this experiment was an A1 size paper, which is mapped to 211 x 149 pixels area. Figure 5.10 shows the simulated path and the actual path of the AGV.

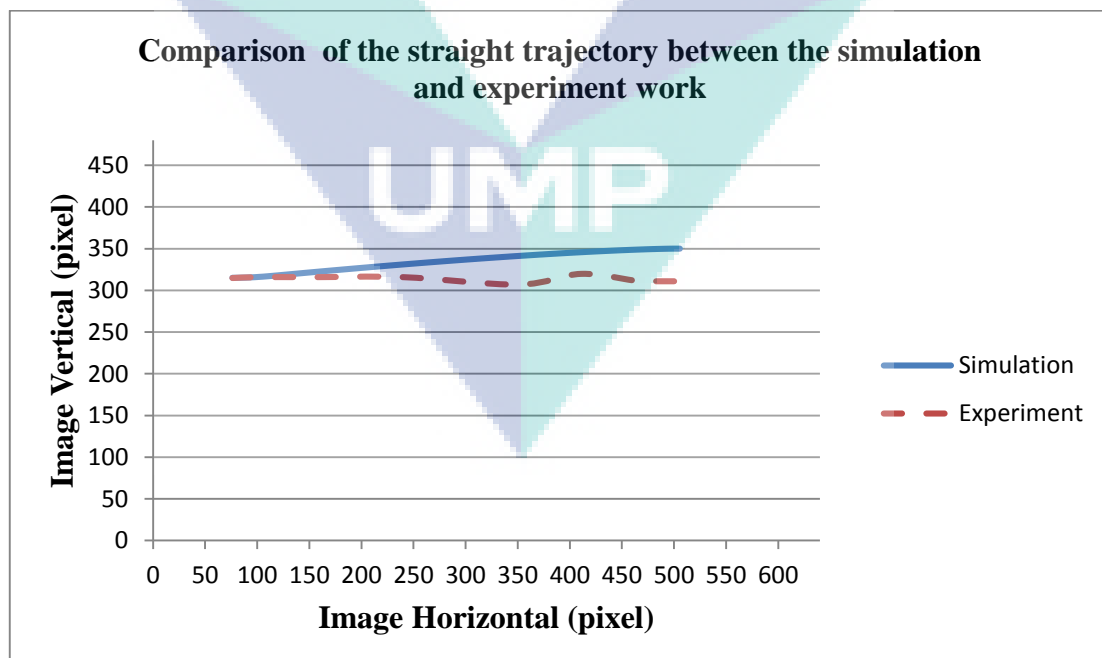
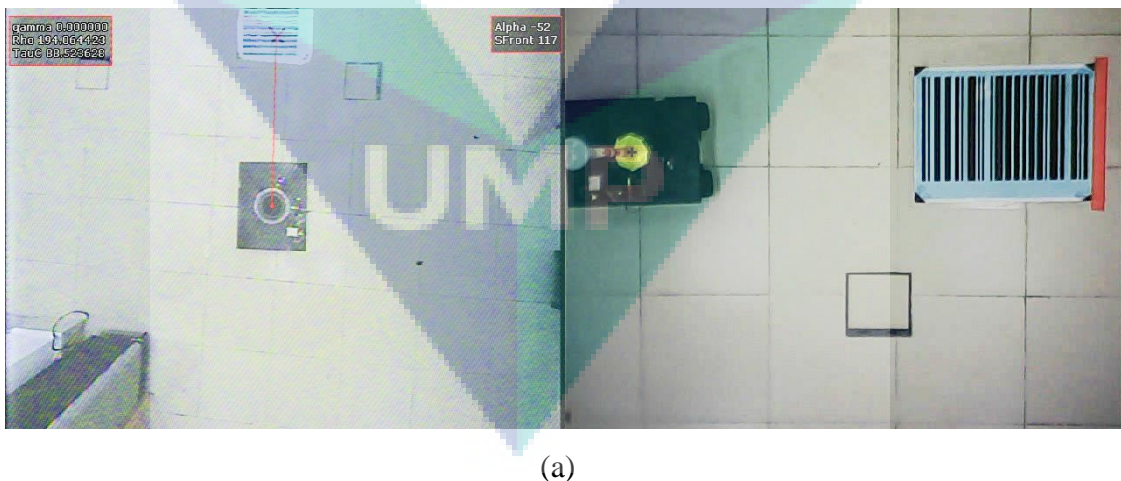


Figure 5.10: Comparison of the straight trajectory between the simulation and experiment

The actual trajectory shows a deviation from the simulated trajectory. The final pose of the AGV in the experiment was (500, 311, -1) while the final pose of in simulation was (500, 350, 0). The AGV had deviated 39 pixels which is an actual distance of 15.6 cm from the simulated final position. A comparison between the experimented data and the simulation data using equations 5.1 to 5.3 showed a residual sum squares error of 6502 pixels² and the standard deviation of 25.5 pixels. The data calculations can be referred to Appendix A. This standard deviation value is 5.3% deviation from the whole tracked vertical position which consist of 480 pixel.

The orientation of the final position only deviate 1° from the centre of the landmark. The final position of the AGV is shown in figure 5.11(c). The left image was captured by the tracking camera and the right image was captured by the AGV camera range sensor.

The progression in the experimental work showed a stray in the region 325 to 450 horizontal pixel. This stray is caused by an obstruction of the view while tracking the base of the camera holder as shown in figure 5.11(b). The obstruction came from the top of the camera as the AGV passed directly under the tracking camera.



(a)

Figure 5.11: Image of the start (a), the middle (b) and the final (c) position for the straight trajectory experiment.

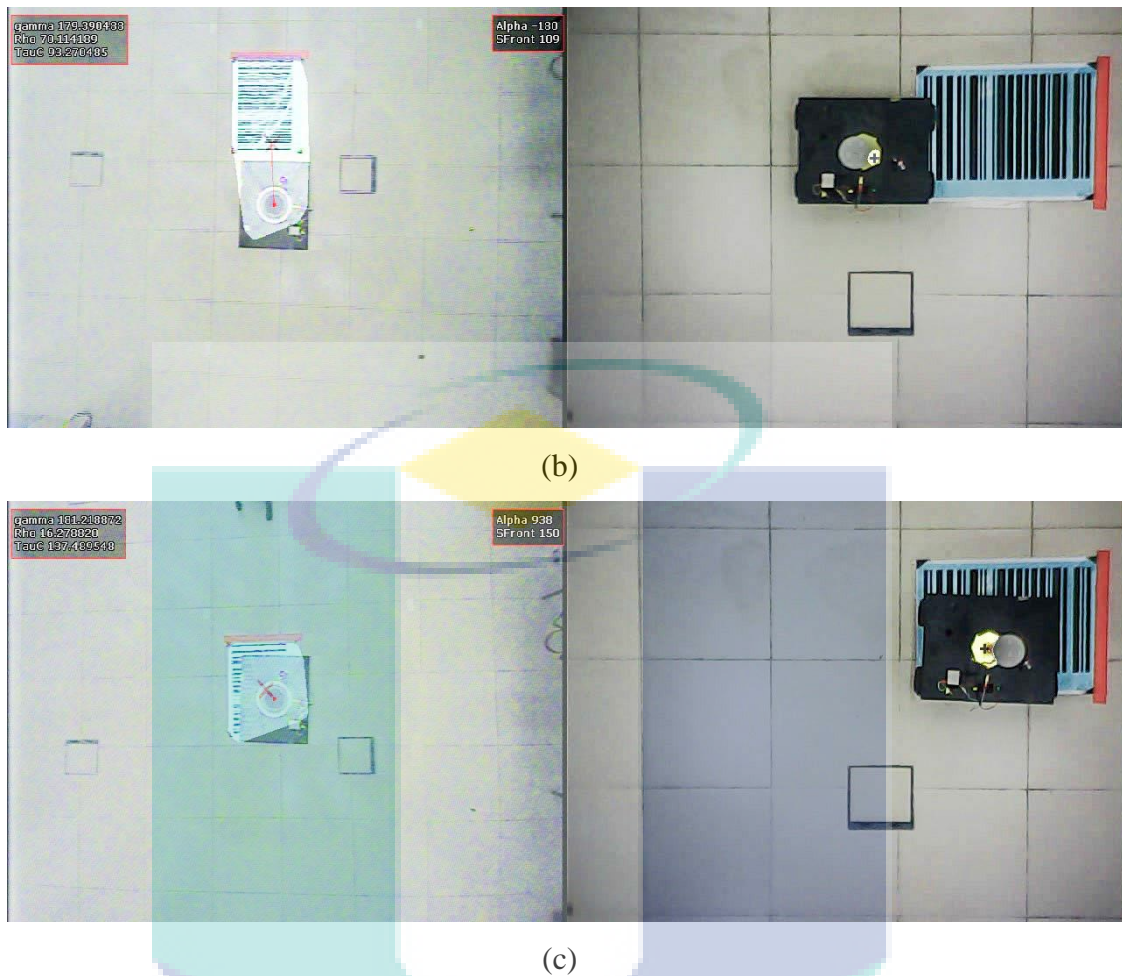


Figure 5.11: continued.

5.3.2 Right turn experiment

In this experiment, the centre of the landmark was placed at (500, 350, 0) pixel coordinate and the AGV was placed at the (153, 74, 91) pixel coordinate. This marks the start position and position of the target. Figure 5.12 shows the simulated and actual path of the AGV. The simulation and the experimental works show a similar progression as the AGV approach the landmarks. However, at 500 horizontal pixel points, the AGV stopped at 405 vertical pixels, while the simulation stopped at 388 vertical pixels.

The deviation between the simulation and the experimental result was 17 pixels, which represent a 6.8 cm in the measurement. However, when the progression is compared between the actual and simulated data, using the equations 5.1 to 5.3, shows a residual sum squares error of 1265 pixel² and the standard deviation of 10.72 pixels. This standard deviation value represented 2.2% of deviation from full 480 vertical image

pixels. The data calculations can be referred to Appendix A. However, just like the side slip test, the absolute data also shows tendency of larger deviation at the end of tracked position compared to the initial position.

On the other hand, the orientation of the final position also must be considered. The final orientation of simulated result was -5.8° while the final position of the experiment was 0° . The final position of the AGV is shown in figure 5.13 (c). The right image was captured by the overhead camera and the left image was captured by the on-board omnidirectional camera.

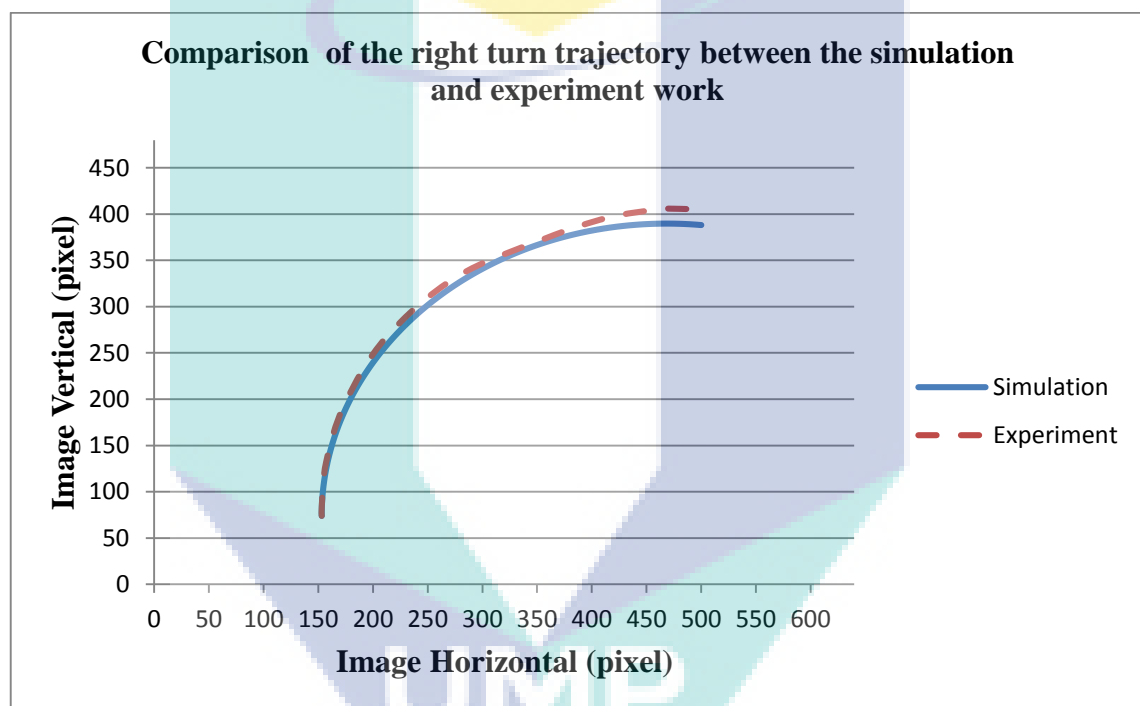


Figure 5.12: Comparison of the right turn trajectory between the simulation and experiment.

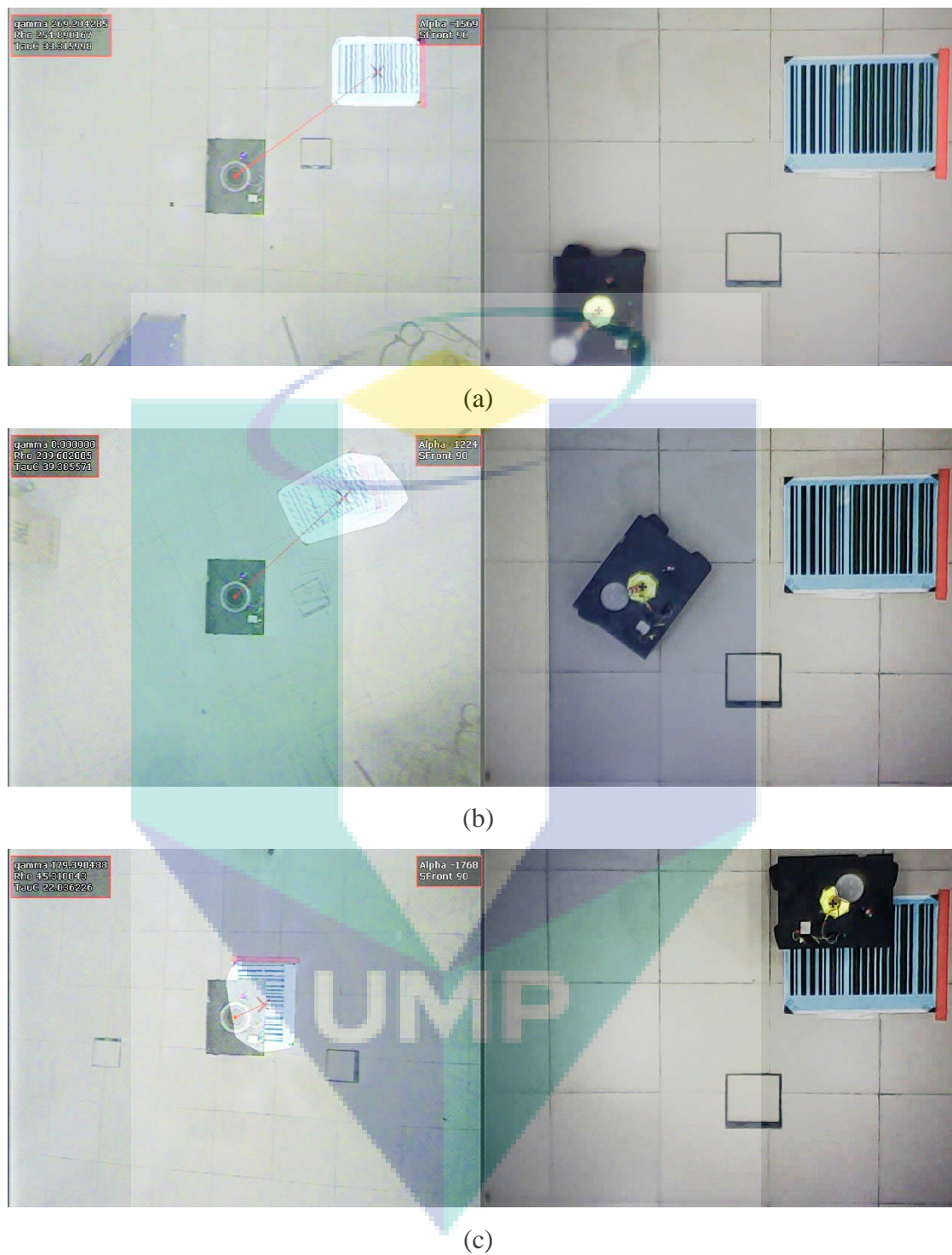


Figure 5.13: Image of the start (a), the middle (b), and the final (c) position for the right turn trajectory experiment.

5.3.3 Left turn experiment

In this experiment, the AGV was placed at the starting pose (610, 74, 86) and the landmark was positioned at (130, 350, 180) both with reference to global coordinate. Figure 5.14 shows the comparison between the simulated and the experimental work. The simulation and the experiment works shows a similar progression as the AGV approach the landmarks. At 130 horizontal pixel points, the simulation shows the vertical pixels at 364 while the experimental work showed that the AGV stopped at 372 vertical pixels.

The deviation between the simulation and the experimental results was 8 pixels, which represent a 3.2 cm in the measurement. However, when the progression is compared between the actual and simulated data, using equations 5.1 to 5.3, a sum of residual squared error showed a value of 3993 pixels² and a standard deviation of 18.24 pixels. This standard deviation value represented 3.8% of deviation from full 480 vertical image pixels. The data calculations can be referred to Appendix A. However, the errors value seems to be consistent at all phases of the experiment; initial middle or final phase.

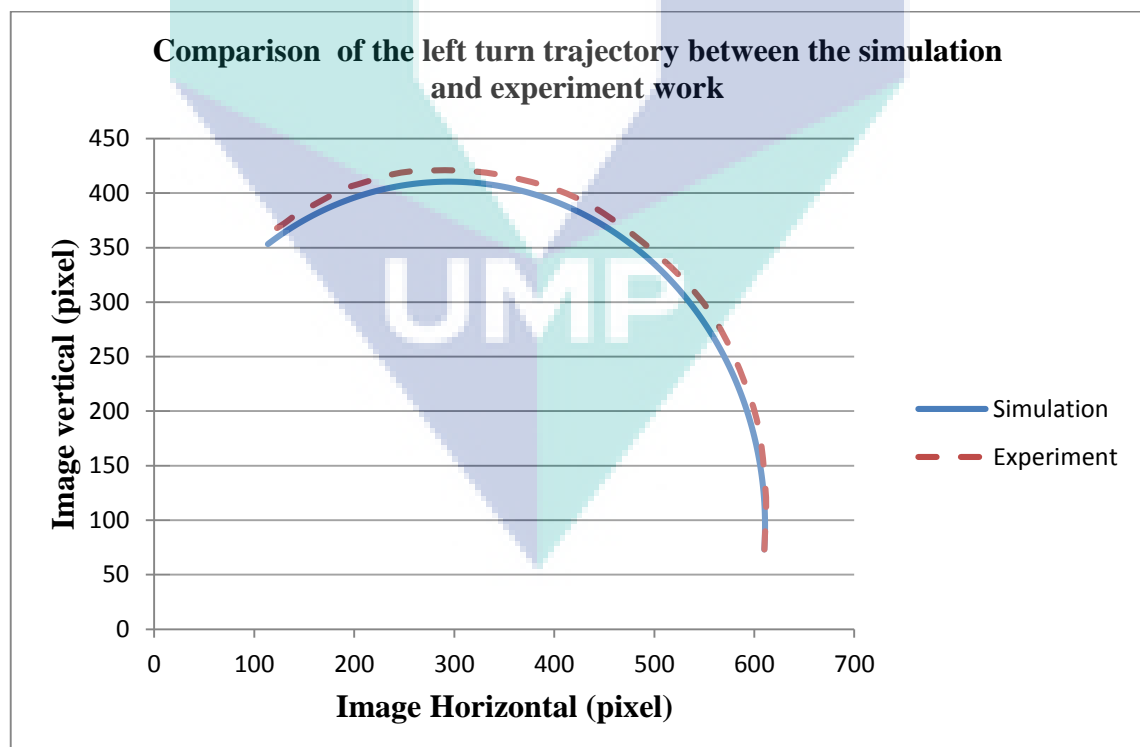


Figure 5.14: Comparison of the left turn trajectory between the simulation and experiment.

The final orientation of simulation work was 211° while the final position of the experiment was 203° . The final position of the AGV is shown in figure 5.15(c). The right image was captured by overhead camera and the left image was captured by the on-board omnidirectional camera.

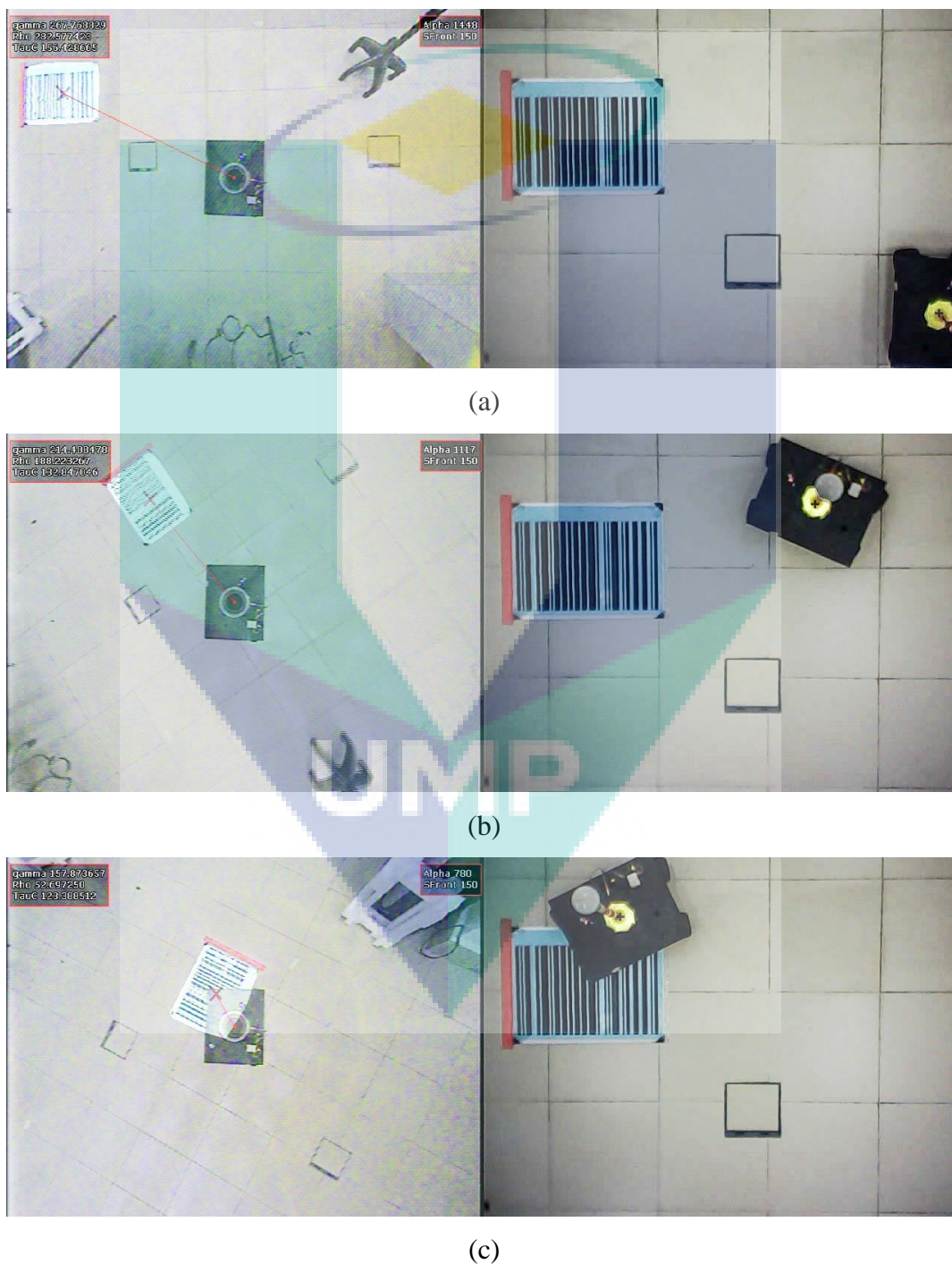


Figure 5.15: Image of the start (a), the middle (b), and the final (c) position for the left turn trajectory experiment

5.3.4 Discussion of the trajectory experiments.

The trajectory experiments forms the basis of the navigation strategy for the AGV to move from a starting point to a final point with the desired final orientation. Similar to the work presented by Chaudhary and Sinha, where they simulate a guided robot arbitrarily close to a point of interest using only range sensors (Chaudhary and Sinha, 2012). However, in this work, the only range sensor used was omnidirectional camera and the point of interest is detected and recognized through image processing of the omnidirectional camera feed.

In this research, the landmark must be in the field of view of the omnidirectional camera before the AGV could make a move. Due to this condition, the omnidirectional camera is very advantageous as it has the widest field of view compared to a single camera. The field of view of the omnidirectional camera covers an area of up to 15.8 m² when mounted at less than 90cm from the ground.

The wide field of view of the camera increases the possibility for the AGV to detect more than one landmark simultaneously. The vision algorithm was programmed to detect landmarks of a specific size. When more than one landmark is detected, the AGV tends to move to the larger of the two. However, the raw image can be segmented before deciding where the AGV should go. The left turn experiment shows the largest deviation from the intended target. This shows that the AGV tends to stop at the side of the landmark. As a matter of fact, in all of the experiments the final pose of the AGV were off-centred from the intended target.

When all data from the three trajectories were compared, it was evident that a steady state error exist. This error may have been resulted from the proportional control used to control steering angle and the speed. Unlike proportional-integral-derivative (PID) control, proportional control feedback did not take into account of the previous error nor the mean error over time in order to control the parameters. A PID control may significantly reduce the steady state error caused by proportional control.

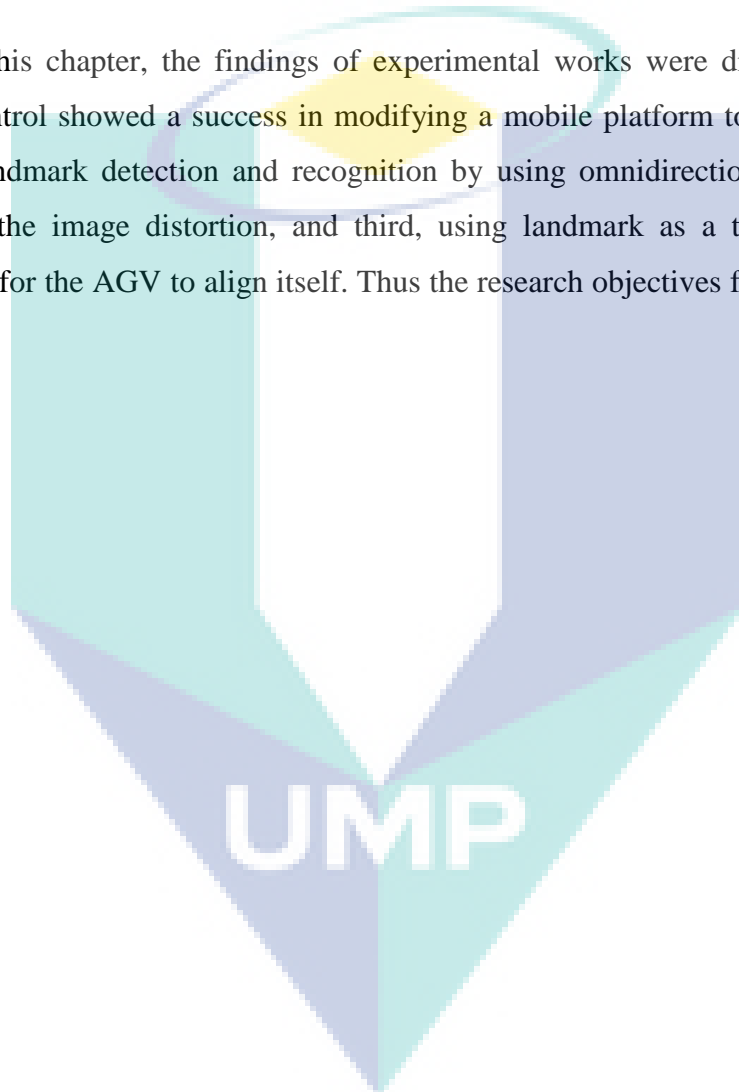
However, implementation of intelligent control to the system such as fuzzy controller may reduce the steady state error further. Chul-Goo Kang and Hee-Sung Kwak had demonstrated the elimination of the steady state position errors in a robotic manipulator by using fuzzy control algorithm (Chul-Goo Kang and Hee-Sung Kwak,

1996). Their work successfully reduce steady state error up to 90% from the two input; position error and velocity error, fuzzy controller.

In this research, only proportional control is used because the primary concern was to generate the trajectory for the AGV to align and position itself with a landmark.

5.4 CHAPTER SUMMARY

In this chapter, the findings of experimental works were discussed. First, the manual control showed a success in modifying a mobile platform to be used as AGV. Second, landmark detection and recognition by using omnidirectional vision without correcting the image distortion, and third, using landmark as a target position and orientation for the AGV to align itself. Thus the research objectives for this research are achieved.



CHAPTER 6

CONCLUSION AND FUTURE WORKS

6.1 SUMMARY OF RESEARCH WORK

The main aim of this research work is to investigate AGV alignment trajectory using catadioptric omnidirectional camera without an image rectification process. The research work started by modifying a mobile robot platform to adopt an omnidirectional camera. Then a suitable landmark pattern is chosen and its detectability and readability was tested. After that the trajectory experiment is conducted. The trajectory experiment is divided into two parts. The first part was a simulation using mathematical model and the second part was experiments using the AGV. In the simulation, the landmark position is given in terms of x-axis, y-axis, and the orientation from x-axis. All simulation work was conducted using MATLAB software. In the second part of the trajectory experiment, the landmark was detected through the omnidirectional camera on board the AGV, and the trajectory was tracked from an overhead camera. The image captured from the omnidirectional camera was processed by a commercially available software, Roborealm. Roborealm software simplified the image processing algorithm by using modules specific to robot building. The result of experiments was presented and discussed in chapter 5.

The first objective of this research is to develop a system using catadioptric omnidirectional camera as the range sensor for an AGV. It has been shown that as the only sensor on board the AGV, the catadioptric camera can provide the position and orientation for the AGV to run in autonomous mode. The advantage of the 360° horizontal view given by the camera allows for an interest point to remain in the camera field of view, even if the AGV is changing its direction. The higher the camera is placed, the further the range the AGV can sense.

The second objective of this research is to use an AGV with catadioptric omnidirectional camera as its range sensor to identify and recognize landmarks for navigation. It has been demonstrated that the landmarks must be salient, distinct and has negligible height. A salient and distinct landmark may be produced from colour contrast or distinct shape and size thus the landmarks identification and recognition process becomes faster even if the landmarks image are distorted by the catadioptric omnidirectional camera. Furthermore the object with negligible height, when viewed through a catadioptric omnidirectional camera, has insignificant distortion. This work then further strengthens a previous finding that the omnidirectional image is only distorted against the height of an object.

The third objective is to successfully generate the trajectory for the AGV to align and position itself with a landmark. In order to align itself with the landmarks, a control system, which control the steering angle and speed of the AGV is needed. It has been shown that even when proportional control was used the errors were less than 6%. The error was mainly steady state error thus using more advanced controller such as PID controller, modern control principal or intelligence control will help reduce the steady state error.

With all three objectives is shown to be achieved, it can thus be concluded that the hypothesis of this research, the AGV can identify and recognize a landmark and navigate to approach the landmark using omnidirectional camera without going through any image rectification process, stand.

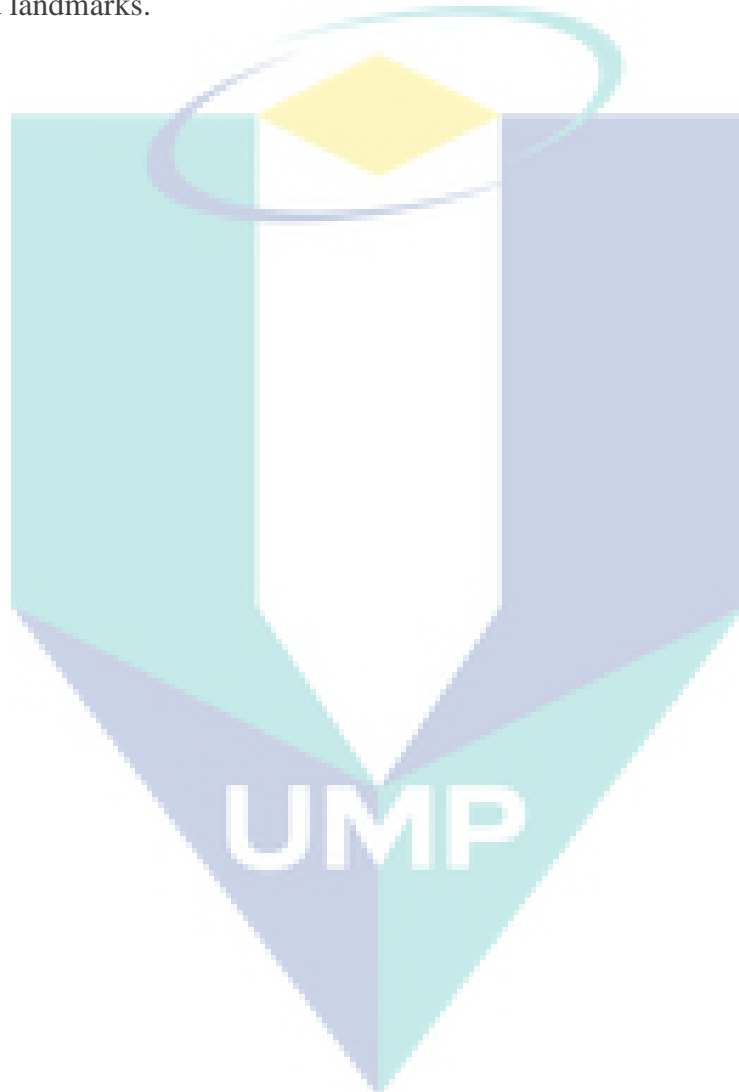
6.2 FUTURE WORK

In this section, several recommendations are put forward. First, the research can be expanded to be conducted in a real manufacturing environment using a standard AGV instead of experiment conduct inside a laboratory. A real manufacturing environment will present further challenges rather than the controlled environment in a laboratory.

Second, as the camera technology becomes more advance the research can be continued using high definition camera. The advantage of high contrast and higher pixel density in high definition camera may lead into the usage of significantly smaller barcoded landmark size. As the landmark becomes smaller, the application of the technology can be more practical as well as in more diverse situation.

Third, the work shall continue to investigate the effect of dynamic illumination in order to detect and recognize the landmarks. This will increase the robustness of the system against different illumination especially caused by natural lighting.

Fourth, the work can be continued to study the control algorithm of the AGV with the application of classical control, modern control or intelligent control. This control algorithm may improve the trajectory of the AGV as well as the accuracy of approaching the targeted landmarks.



REFERENCES

- AIXUE, Y., HAIBING, Z., ZHENG DONG, X., CHENXI, S. & KUI, Y. A vision-based guidance method for autonomous guided vehicles. *Mechatronics and Automation (ICMA)*, 2012 International Conference on, 5-8 Aug. 2012 2012. 2025-2030.
- ANDERSEN, G. I., CHRISTENSEN, A. C. & RAVN, O. Augmented models for improving vision control of a mobile robot. *Control Applications*, 1994., Proceedings of the Third IEEE Conference on, 1994. 53-58 vol.1.
- BEINHOFER, M., MULLER, J. & BURGARD, W. Near-optimal landmark selection for mobile robot navigation. *Robotics and Automation (ICRA)*, 2011 IEEE International Conference on, 9-13 May 2011 2011. 4744-4749.
- BONIN-FONT, F., ORTIZ, A. & OLIVER, G. 2008. Visual navigation for mobile robots: A survey. *Journal of Intelligent and Robotic Systems: Theory and Applications*, 53, 263-296.
- BRIGGS, A. J., SCHARSTEIN, D., BRAZIUNAS, D., DIMA, C. & WALL, P. Mobile robot navigation using self-similar landmarks. 2000. 1428-1434.
- BUXTON, B. F., CASTELOW, D. A., RYGOL, M., MCLAUCHLAN, P. F. & POLLARD, S. B. Developing a stereo vision system for control of an AGV. *Design and Application of Parallel Digital Processors*, 1991., Second International Specialist Seminar on the, 15-19 Apr 1991 1991. 79-83.
- CHAUDHARY, G. & SINHA, A. Detecting a target location using a mobile robot with range only measurement. *Industrial Electronics and Applications (ICIEA)*, 2012 7th IEEE Conference on, 18-20 July 2012 2012. 28-33.
- CHUL-GOO KANG & HEE-SUNG KWAK. A fuzzy control algorithm reducing steady-state position errors of robotic manipulators. *Advanced Motion Control*, 1996. AMC '96-MIE. Proceedings., 1996 4th International Workshop on, 1996. 121-126 vol.1.
- CONGIU, S., ORSENIGO, L. & PAGELIO, E. Navigation and manipulation in an unstructured power plant environment. *Industrial Electronics, Control and Instrumentation*, 1994. IECON '94., 20th International Conference on, 5-9 Sep 1994 1994. 958-962 vol.2.
- CUCCHIARA, R., PERINI, E. & PISTONI, G. Efficient Stereo Vision for Obstacle Detection and AGV Navigation. *Image Analysis and Processing*, 2007. ICIAP 2007. 14th International Conference on, 10-14 Sept. 2007 2007. 291-296.
- DANWEI, W. & FENG, Q. Trajectory planning for a four-wheel-steering vehicle. *Robotics and Automation*, 2001. Proceedings 2001 ICRA. IEEE International Conference on, 2001 2001. 3320-3325 vol.4.
- DESOUZA, G. N. & KAK, A. C. 2002. Vision for mobile robot navigation: A survey. *IEEE Transactions on Pattern Analysis and Machine Intelligence*, 24, 237-267.
- DONGKYOUNG, C. 2004. Sliding-mode tracking control of nonholonomic wheeled mobile robots in polar coordinates. *Control Systems Technology, IEEE Transactions on*, 12, 637-644.
- ESPARZA, D. & SAVAGE, J. Topological Mobile Robot Navigation Using Artificial Landmarks. *Robotics Symposium and Competition (LARS/LARC)*, 2013 Latin American, 21-27 Oct. 2013 2013. 38-42.

- FIALA, M. Linear markers for robot navigation with panoramic vision. *Computer and Robot Vision*, 2004. Proceedings. First Canadian Conference on, May 17-19, 2004 2004. 145-154.
- FLORCYZK, S. 2005. *Robot Vision: Video-based Indoor Exploration with Autonomous and Mobile Robots* Weinheim, WILEY-VCH Verlag GmbH & Co. KGaA,.
- GOLNABI, H. 2003. Role of laser sensor systems in automation and flexible manufacturing *Robotics and Computer Intergrated Manufacturing* 19, 201-210.
- GUANGHUI, L. & ZHIJIAN, J. An artificial landmark design based on mobile robot localization and navigation. 2011. 588-591.
- GUO, L. X., FAN, K. & YAN, W. J. 2013. Localization and map building of laser sensor AGV based on Kalman filter.
- GÜZEL, M. S. 2013. Autonomous vehicle navigation using vision and mapless strategies: A survey. *Advances in Mechanical Engineering*, 2013.
- HER, M. G., LIANG, W. J., WU, K. W., PENG, C. C., HSU, K. S. & PENG, Y. C. 2013. Development of a vision guided mobile robot and its applications in automated production lines.
- HUANG HONG & TING ZHANG. Mobile robot trajectory tracking on adaptive binocular vision and fuzzy control. *Control and Decision Conference*, 2009. CCDC '09. Chinese, 2009. 632-635.
- ILAS, C. Perception in autonomous ground vehicles. *Electronics, Computers and Artificial Intelligence (ECAI)*, 2013 International Conference on, 27-29 June 2013 2013. 1-6.
- JANG, G., KIM, S., LEE, W. & KWEON, I. Color landmark based self-localization for indoor mobile robots. 2002. 1037-1042.
- JIN WOO, L., JUNG HO, K., YOUNG JIN, L. & KWON SOON, L. A study on recognition of lane and movement of vehicles for port AGV vision system. *Industrial Electronics*, 2002. ISIE 2002. Proceedings of the 2002 IEEE International Symposium on, 2002 2002. 463-466 vol.2.
- JUN, Y., PEIHUANG, L., XIAOMING, Q. & XING, W. An Intelligent Real-Time Monocular Vision-Based AGV System for Accurate Lane Detecting. *Computing, Communication, Control, and Management*, 2008. CCCM '08. ISECS International Colloquium on, 3-4 Aug. 2008 2008. 28-33.
- JUNG-MIN, Y. & JONG-HWAN, K. 1999. Sliding mode control for trajectory tracking of nonholonomic wheeled mobile robots. *Robotics and Automation, IEEE Transactions on*, 15, 578-587.
- KAY, M. G. & LUO, R. C. Global vision for the control of free-ranging AGV systems. *Robotics and Automation*, 1993. Proceedings., 1993 IEEE International Conference on, 2-6 May 1993 1993. 14-19 vol.2.
- KELLY, A., NAGY, B., STAGER, D. & UNNIKRISHNAN, R. 2007. Field and service applications - An infrastructure-free automated guided vehicle based on computer vision - An Effort to Make an Industrial Robot Vehicle that Can Operate without Supporting Infrastructure. *Robotics & Automation Magazine, IEEE*, 14, 24-34.
- KNIGHT, J. & REID, I. Active visual alignment of a mobile stereo camera platform. *Robotics and Automation*, 2000. Proceedings. ICRA '00. IEEE International Conference on, 2000 2000. 3203-3208 vol.4.
- LEE, D. H., SUN, J. S., HAN, S. B., PARK, C. S. & KIM, J. H. 2008. Omnidirectional robot system and localization for fira robot. *Journal of Harbin Institute of Technology (New Series)*, 15, 96-99.

- LIN, W., JIA, S., YANG, F. & TAKASE, K. Topological navigation of mobile robot using ID tag and web camera. *Intelligent Mechatronics and Automation*, 2004. Proceedings. 2004 International Conference on, 2004. IEEE, 644-649.
- LU, W., HUI, G. & ZIXING, C. Topological Mapping and Navigation for Mobile Robots with Landmark Evaluation. *Information Engineering and Computer Science*, 2009. ICIECS 2009. International Conference on, 19-20 Dec. 2009 2009. 1-5.
- MARTÍN, A. & ADÁN, A. 2012. 3D real-time positioning for autonomous navigation using a nine-point landmark. *Pattern Recognition*, 45, 578-595.
- MARTÍNEZ-BARBERÁ, H. & HERRERO-PÉREZ, D. 2010. Autonomous navigation of an automated guided vehicle in industrial environments. *Robotics and Computer-Integrated Manufacturing*, 26, 296-311.
- MATA, M., ARMINGOL, J. M., DE LA ESCALERA, A. & SALICHS, M. A. A visual landmark recognition system for topological navigation of mobile robots. 2001. 1124-1129.
- MILJKOVIĆ, Z., VUKOVIĆ, N., MITIĆ, M. & BABIĆ, B. 2013. New hybrid vision-based control approach for automated guided vehicles. *International Journal of Advanced Manufacturing Technology*, 66, 231-249.
- MORAVEC, H. P. 1983. STANFORD CART AND THE CMU ROVER. *Proceedings of the IEEE*, 71, 872-884.
- PETRIU, E. M., TRIF, N., MCMATH, W. S. & YEUNG, S. K. Environment encoding for AGV navigation using vision. *Vehicle Navigation and Information Systems Conference*, 1993., Proceedings of the IEEE-IEE, 12-15 Oct 1993 1993. 525-528.
- PING, K., QINXING, Z. & XUDONG, C. A Road Lane Recognition Algorithm Based on Color Features in AGV Vision Systems. *Communications, Circuits and Systems Proceedings*, 2006 International Conference on, June 2006 2006. 475-479.
- RATNER, D. & MCKERROW, P. 2003. Navigating an outdoor robot along continuous landmarks with ultrasonic sensing. *Robotics and Autonomous Systems*, 45, 73-82.
- RUI ZHAO & JIAN FANG. The Path Recognition System Design of the Mobile Robot Based on the Vision Navigation. *Computer, Consumer and Control (IS3C)*, 2014 International Symposium on, 2014. 419-421.
- SABIKAN, S., SULAIMAN, M., SALIM, S. N. S. & MISKON, M. F. 2010. Vision Based Automated Guided Vehicle for Navigation and Obstacle Avoidance. *Proceeding of the 2nd International Conference on Engineering and ICT*.
- SHIMIZUHIRA, W., FUJII, K. & MAEDA, Y. Fuzzy behavior control for autonomous mobile robot in dynamic environment with multiple omnidirectional vision system. *Intelligent Robots and Systems*, 2004. (IROS 2004). Proceedings. 2004 IEEE/RSJ International Conference on, 2004. 3412-3417 vol.4.
- SIEGWART, R. & NOURBAKHSH, I. R. 2004. *Introduction to Autonomous Mobile Robots*, Cambridge, Massachusetts
London, England The MIT Press.
- SOLEA, R., FILIPESCU, A., MINZU, V. & FILIPESCU, S. Sliding-mode trajectory-tracking control for a four-wheel-steering vehicle. *Control and Automation (ICCA)*, 2010 8th IEEE International Conference on, 9-11 June 2010 2010. 382-387.
- SONGMIN, J., WEI, C., XIUZHI, L., HONGMIN, S. & JINBO, S. Mobile robot 3D map building based on laser ranging and stereovision. *Mechatronics and Automation (ICMA)*, 2011 International Conference on, 7-10 Aug. 2011 2011. 1774-1779.

- SPAMPINATO, G., LIDHOLM, J., AHLBERG, C., EKSTRAND, F., EKSTROM, M. & ASPLUND, L. An embedded stereo vision module for industrial vehicles automation. *Industrial Technology (ICIT), 2013 IEEE International Conference on*, 25-28 Feb. 2013. 52-57.
- STORJOHANN, K., ZIELKE, T., MALLOT, H. A. & VON SEELEN, W. Visual obstacle detection for automatically guided vehicles. *Robotics and Automation, 1990. Proceedings., 1990 IEEE International Conference on*, 13-18 May 1990. 761-766 vol.2.
- T.TAYLOR, S. G., W.W.BOLES 2004. Monocular Vision as a Range Sensor. *In: MOHAMMADIAN, M. (ed.) International Conference on Computational Intelligence for Modelling Control and Automation (CIMCA 2004)*. Gold Coast, Australia.
- TAHA, Z., CHEW, J. Y. & YAP, H. J. 2010. Omnidirectional vision for mobile robot navigation. *Journal of Advanced Computational Intelligence and Intelligent Informatics*, 14, 55-62.
- TAHA, Z. & JIZAT, J. A. M. 2012. A comparison of two approaches for collision avoidance of an automated guided vehicle using monocular vision.
- TONG, F., TSO, S. K. & XU, T. Z. 2005. A high precision ultrasonic docking system used for automatic guided vehicle. *Sensors and Actuators, A: Physical*, 118, 183-189.
- UCHIBE, E., ASADA, M. & HOSODA, K. Environmental complexity control for vision-based learning mobile robot. *Robotics and Automation, 1998. Proceedings. 1998 IEEE International Conference on*, 1998. 1865-1870 vol.3.
- WEIJIA, F., YULI, L. & ZUOLIANG, C. Omnidirectional vision tracking and positioning for vehicles. 2008. 183-187.
- XIE, M. 1995. Trinocular vision for AGV guidance: Path localization and obstacle detection. *Computers & Electrical Engineering*, 21, 441-452.
- XIUZHI LI, SONGMIN JIA, JINHUI FAN, LIWEN GAO & BING GUO. Autonomous mobile robot guidance based on ground line mark. *SICE Annual Conference (SICE), 2012 Proceedings of*, 2012. 1091-1095.
- XU, L. & TIAN, Z. 2011. Design for AGV based on binocular stereo vision.
- YAN, X. Z., WANG, S. X., MA, Z. S. & LI, X. 2006. Automatic guided vehicle system based on localization and navigation by ultrasonic and infrared ray. *Jilin Daxue Xuebao (Gongxueban)/Journal of Jilin University (Engineering and Technology Edition)*, 36, 242-246.
- YINGJIE, S., QIXIN, C. & WEIDONG, C. An object tracking and global localization method using omnidirectional vision system. *Intelligent Control and Automation, 2004. WCICA 2004. Fifth World Congress on*, 15-19 June 2004. 4730-4735 Vol.6.
- YU, Z., YIN, X., CAO, Z., YAO, B., LIU, G. & ZHAO, H. 2013. Design of the control system for laser guiding AGV.
- ZHANG, H., ZHANG, L. & DAI, J. Landmark-based localization for indoor mobile robots with stereo vision. 2012. 700-702.
- ZIAIE-RAD, S., JANABI-SHARIFI, F., DANESH-PANAH, M. M., ABDOLLAHI, A., OSTADI, H. & SAMANI, H. A practical approach to control and self-localization of Persia omni directional mobile robot. *Intelligent Robots and Systems, 2005. (IROS 2005). 2005 IEEE/RSJ International Conference on*, 2005. 3473-3479.

APPENDIX A
STATISTICS DATA CALCULATION FOR THE TRAJECTORIES

Change lane					MEAN Error	7.17
	SIM	EXP	Err	Err^2		
100	100	100	0	0		
116	100	103	3	9		
170	105	110	5	25		
260	137	138	1	1		
368	230	220	-10	100		
455	334	336	2	4		
514	376	385	9	81		
530	385	395	10	100		
574	403	415	12	144		
612	412	427	15	225		
649	417	435	18	324		
675	417	438	21	441		
			RSE	1454		
			VAR	121.17		
			STDEV	11.01		
Straight					MEAN error	-19.600
X	SIM	EXP	Error	Err^2		
76	315	315	0	0		
77	315	315	0	0		
101	316	316	0	0		
154	322	316	-6	36		
240	331	316	-15	225		
351	341	307	-34	1156		
411	346	320	-26	676		
466	349	311	-38	1444		
477	349	311	-38	1444		
500	350	311	-39	1521		
			RSE	6502		
			VAR	650.2		
			STDEV	25.50		

**APPENDIX A
(CONTINUED)**

Right turn					MEAN error	8.273
X	EXP	SIM	ERR	Err^2		
153	74	74	0	0		
153	84	91	-7	49		
157	132	124	8	64		
174	195	188	7	49		
212	267	258	9	81		
276	332	324	8	64		
358	374	368	6	36		
414	396	385	11	121		
459	405	389	16	256		
467	406	390	16	256		
500	405	388	17	289		
	11		RSE	1265		
			VAR	115		
			STDEV	10.72		
Left turn					MEAN error	15.083
COG_X	SIM	EXP	Error	Err^2		
610	73	73	0	0		
611	97	129	32	1024		
597	187	209	22	484		
545	287	304	17	289		
443	347	385	38	1444		
349	406	416	10	100		
260	409	420	11	121		
204	397	408	11	121		
184	390	401	11	121		
144	372	381	9	81		
130	364	372	8	64		
118	353	365	12	144		
		12	RSE	3993		
			VAR	332.75		
			STDEV	18.24		

APPENDIX B

ON BOARD AGV ARDUINO PROGRAM

```

#include <Servo.h>    //library used

String MyString;    // create string object
Servo myservoa, myservob; // create servo object to control a servo

void setup() {
  Serial.begin(115200);
  pinMode(4, OUTPUT); //Pin for Motor direction M1 DFRdriver
  pinMode(6, OUTPUT); //Pin for Motor direction M2 DFRdriver
  pinMode(5, OUTPUT); //Pin for Motor Speed M1 DFRdriver
  pinMode(7, OUTPUT); //Pin for Motor Speed M2 DFRdriver
  myservoa.attach(11); //the pin for the servoa signal
  myservob.attach(10); //the pin for the servob control
  myservoa.write(120); //Set servoa initial position.
  myservob.write(120); //Set servoa initial position.
}
void loop()
{
  if (Serial.available())
  {
    char c = Serial.read(); //gets one byte from serial buffer
    if (c == ',')
    {
      if (MyString.length() >1)
      {
        int n = MyString.toInt(); //convert MyString into a number
        Serial.println(n); //print value of n (index of character)
        if(MyString.indexOf('a') >0) myservoa.write(n);
        if(MyString.indexOf('b') >0) myservob.write(n);
        if(MyString.indexOf('z') >0) // Forward control index
        {
          digitalWrite(4,HIGH); //
          analogWrite(5, n);
          digitalWrite(7,HIGH); //
          analogWrite(6, n);
        }
        if(MyString.indexOf('y') >0) // Reverse control Index
        {
          digitalWrite(4,LOW);
          analogWrite(5, n);
          digitalWrite(7,LOW);
          analogWrite(6, n);
        }
      }
      MyString=""; //clears variable for new input
    }
    else
    {
      MyString += c; //makes the string MyString
    }
  }
}

```

APPENDIX C

ROBOREALM CSCRIPT PROGRAM

```

int gamma = getVariable("gamma");
int tauc = getVariable("TauC");
int rho = getVariable("Rho");
int factor = 5;
int cogX = getVariable("COG_X");
int B1 = 0;

int B2 = 90;
int Gang;
int RotA;
int forward;
int reverse;
int Sfront= 120;
int Sback=120 ;
float Kp=3.0;
int Ks=25;
int Kt=-1;

Gang = B2 - B1;
if(Gang>=0)
{
    B1=B2-gamma;
}
else
{
    B1=180-gamma+B2;
}

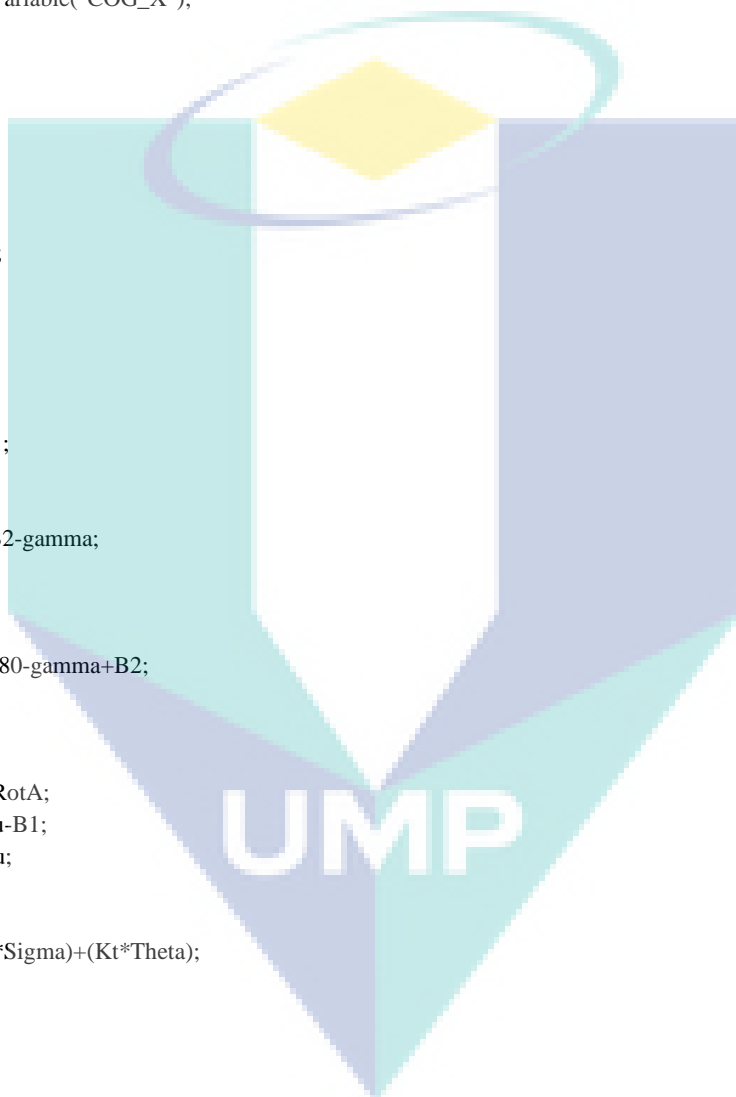
RotA = 90-B1;
int Tau = tauc-RotA;
int Sigma = Tau-B1;
int Theta = -Tau;

int v = Kp*rho;
int alpha = (Ks*Sigma)+(Kt*Theta);

if(cogX!=0)
{
    forward = v/factor;
    if(forward > 254)
    {
        forward=255;
    }

    int alef= alpha/16;
    Sfront = 120+alef;
    if(Sfront>150)
    {
        Sfront=150;
    }
}

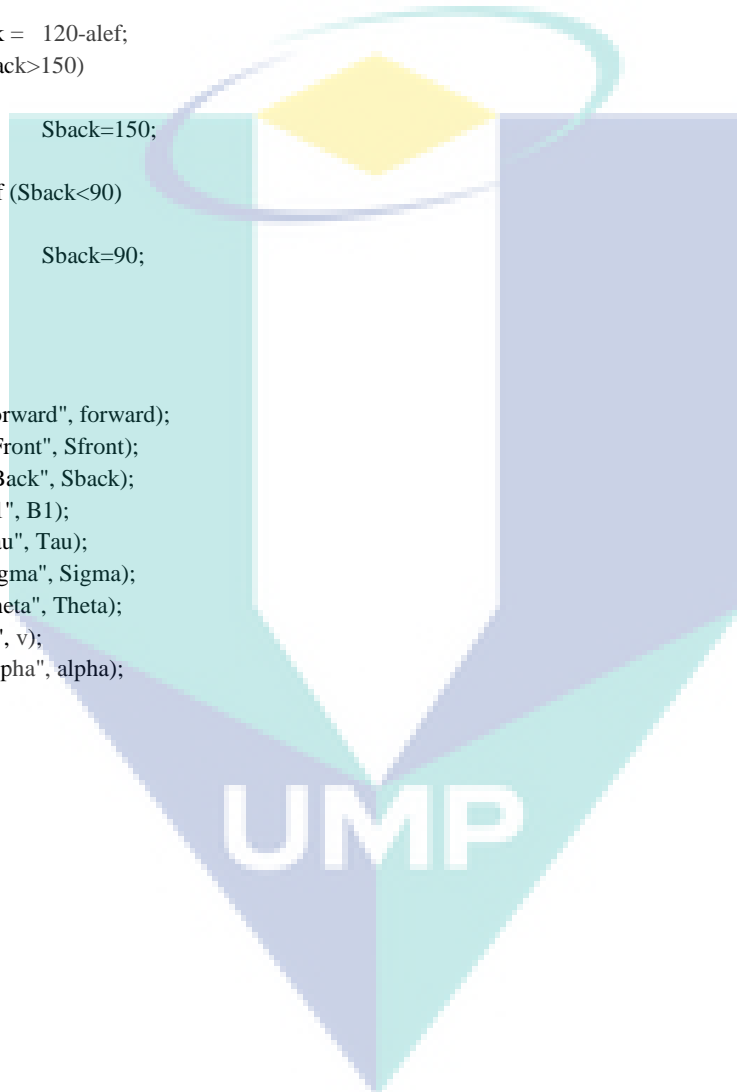
```



APPENDIX C
(CONTINUED)

```
else if(Sfront<90)
{
    Sfront=90;
}
Sback = 120-alef;
if(Sback>150)
{
    Sback=150;
}
else if (Sback<90)
{
    Sback=90;
}
}

setVariable("Forward", forward);
setVariable("SFront", Sfront);
setVariable("SBack", Sback);
setVariable("B1", B1);
setVariable("Tau", Tau);
setVariable("Sigma", Sigma);
setVariable("Theta", Theta);
setVariable("V", v);
setVariable("Alpha", alpha);
```



APPENDIX D
LIST OF PUBLICATIONS

Taha, Z.; Mat-Jizat, J.A.,

"Landmark navigation in low illumination using omnidirectional camera,"

Ubiquitous Robots and Ambient Intelligence (URAI), 2012 9th International Conference on , vol., no., pp.262,265, 26-28 Nov. 2012

doi: 10.1109/URAI.2012.6462990

Taha, Z., Mat-Jizat, J.A., Ishak, I.

Bar code detection using omnidirectional vision for automated guided vehicle navigation

(2012) IET Conference Publications 2012 (598 CP) PP. 589 - 592

doi: 10.1049/cp.2012.1048

Taha, Z., Jizat, J.A.M.

A comparison of two approaches for collision avoidance of an automated guided vehicle using monocular vision

(2012) Applied Mechanics and Materials 145 PP. 547 - 551

doi: 10.4028/www.scientific.net/AMM.145.547

UMP